

OAK RIDGE NATIONAL LABORATORY LIBRARIES
3 4456 0548551 5

CENTRAL RESEARCH LIBRARY
DOCUMENT COLLECTION

LABORATORY

operated by
UNION CARBIDE CORPORATION
for the
U.S. ATOMIC ENERGY COMMISSION



ORNL - TM - 1053

17

ENVIRONMENTAL STUDIES: RADIOLOGICAL SIGNIFICANCE
OF
NUCLEAR ROCKET DEBRIS

SEMI-ANNUAL PROGRESS REPORT
FOR
PERIOD JULY 1 - DECEMBER 31, 1964
(Title Unclassified)

- B. R. Fish
- R. H. Boyett
- T. G. Clark
- J. L. Thompson
- W. H. Wilkie, Jr.

HEALTH PHYSICS DIVISION

Classification Cancelled
Or Changed To
By Authority Of ACE 9/13/71
By Spelling Date 11/16/71

CENTRAL RESEARCH LIBRARY
DOCUMENT COLLECTION
LIBRARY LOAN COPY
DO NOT TRANSFER TO ANOTHER PERSON
If you wish someone else to see this document, send in name with document and the library will arrange a loan.



LEGAL NOTICE

This report was prepared as an account of Government sponsored work. Neither the United States, nor the Commission, nor any person acting on behalf of the Commission:

- A. Makes any warranty or representation, expressed or implied, with respect to the accuracy, completeness, or usefulness of the information contained in this report, or that the use of any information, apparatus, method, or process disclosed in this report may not infringe privately owned rights; or
- B. Assumes any liabilities with respect to the use of, or for damages resulting from the use of any information, apparatus, method, or process disclosed in this report.

As used in the above, "person acting on behalf of the Commission" includes any employee or contractor of the Commission, or employee of such contractor, to the extent that such employee or contractor of the Commission, or employee of such contractor prepares, disseminates, or provides access to, any information pursuant to his employment or contract with the Commission, or his employment with such contractor.

[REDACTED]

ORNL-TM-1053

ENVIRONMENTAL STUDIES: RADIOLOGICAL SIGNIFICANCE
OF
NUCLEAR ROCKET DEBRIS*

SEMI-ANNUAL PROGRESS REPORT
FOR
PERIOD JULY 1 - DECEMBER 31, 1964
(Title Unclassified)

B. R. Fish
R. H. Boyett
T. G. Clark
J. L. Thompson
W. H. Wilkie, Jr.

HEALTH PHYSICS DIVISION

APRIL 1965

* For Space Nuclear Propulsion Office, United States Atomic Energy
Commission, National Aeronautics and Space Administration.

[REDACTED]



3 4456 0548551 5

CONTENTS

	Page
1.0 INTRODUCTION	1
2.0 COMPUTER PROGRAM	2
3.0 DOSIMETRY TECHNIQUES	6
3.1 Introduction	6
3.2 Extrapolation Chamber	7
3.3 Film Dosimeters	7
3.4 Lithium Fluoride Dosimetry	11
3.5 β - γ Flux-Spectra Measurements	11
4.0 EXAMINATION OF REACTOR DEBRIS PARTICLES FROM NRX-A2 TEST	13
4.1 Introduction	13
4.2 Particle Description	13
4.3 Dose Estimates	13
4.4 Particle β - γ Spectra	16
4.4.1 Gamma Spectra	16
4.4.2 β -Spectrum	16
4.5 Radioisotope Content	21
4.5.1 Estimation of $^{140}\text{Ba-La}$ and of $^{95}\text{Zr-Nb}$	21
4.5.2 Comparison with Calculated Inventory	21
5.0 PRODUCTION OF SPHERICAL PARTICLES	25
5.1 Carnuba Wax Particles	25
5.1.1 Particle Description	25
5.1.2 Spheroidizing Technique	26
5.2 Graphite Particles	26
5.2.1 Particle Composition	26
5.2.2 Spheroidizing Technique	29

	Page
6.0 EXPOSURE OF GASTROINTESTINAL TRACT TO "INSOLUBLE" BETA-EMITTERS	29
6.1 Effects of Radiation on the GI Tract-Literature Review	29
6.2 Transit of Insoluble Particles through the GI Tract	35
6.3 Retention of Small Particles in the GI Tract and Their Proximity to the Wall During Transit	36
7.0 EXPOSURE OF SKIN TO DISCRETE PARTICLE SOURCES	39
7.1 Introduction	39
7.2 Initial Deposition of Particles Falling on the Skin	39
7.3 Retention of Particles on Human Skin	39
7.3.1 Introduction	39
7.3.2 Retention of Wax Particles on Skin	39
8.0 SOLUBILITY	43
9.0 TRIPS AND MEETINGS	43
10.0 REFERENCES	45

ENVIRONMENTAL STUDIES: RADIOLOGICAL SIGNIFICANCE
OF NUCLEAR ROCKET DEBRIS

1.0 INTRODUCTION

Radiological safety studies are being conducted for the Space Nuclear Propulsion Office, Flight Safety Branch. This work is concerned primarily with the health physics significance of radioactive debris which may enter the earth biosphere as a result of accidental or operational fragmentation of a nuclear rocket reactor after powered operation. The major emphasis of the program is on the β - γ dosimetry of small, discrete particle sources in contact with the lining of the gastrointestinal tract or lying on the skin.^(1, 2)

The computer program for β - γ dose calculations^(4, 5) has been revised to include slab sources in addition to spherical sources. Further extensions of the program permit plotting of isodose lines and the determination of dose averages over finite areas, e. g., averaged over 1 cm². The revised program is written in FORTRAN-4 for the CDC-1604 computer (ZAP 3. 1) and for the IBM-7090 computer (ZAP 3. 2).

Experimental dose measurements of activated fuel fragments and of spiked, simulated debris particles are based on three dosimetric techniques. Most of the dose measurements have been made with lithium-fluoride thermoluminescent dosimeters,⁽³⁾ although a few baseline measurements have been made with an extrapolation chamber. X-ray film is used to examine the uniformity of the emission flux from sources and to determine the shape of isodose lines. Beta- and gamma-emission flux and energy spectra are measured with anthracene and with sodium-iodide crystal spectrometers.

Reactor debris particles were obtained from the NRX-A2 operation of September 24, 1964. Dose rates and beta and gamma flux and energy spectra are being measured as a function of time. In addition, the quantities of identifiable gamma-emitters are determined for comparison with existing computer estimates of fission product inventory.

Spherical particles in the range 50 to 1000 microns diameter are being made by two techniques. In both procedures a tracer is added to a matrix which is sized

roughly by comminution and sieving. Fragments of low-temperature melting matrices are spheroidized by settling through a temperature gradient. Other materials are formed into spheres by abrasive grinding. Particles spiked with radionuclides are used in making baseline dose measurements in air and in tissue-equivalent absorbers.⁽³⁾

Fluorescent tracers are added to particles used in studying the transit of insoluble particles through the gastrointestinal tract and in studies of particle adhesion to skin.

2.0 COMPUTER PROGRAM

ZAP, a program designed to estimate radiation dose rates from small spherical sources as a function of tissue depth, is described in previous reports.^(3,4,5) Although serious deficiencies exist in the basic premises used in ZAP, no better system is available, at present, for quickly obtaining first-order estimates of depth doses. Improvements have been made in data input formats, and the program has been rewritten in FORTRAN-4 for the 7090 computer. This version, ZAP 3.2, requires the maximum storage capabilities of the 7090 system and has no provision for automatic data plotting. Consequently, ZAP 3.1, written in FORTRAN 63 for the CDC-1604 computer, is at present the system of choice for routine dose calculations. Dose rate data may be read out of the computer in any or all of three formats. Figure 2.1 is an example of one output format listing dose rate (RAD/second) at preselected points in an absorber. Similarly, this output mode will tabulate derived beta- and gamma-flux spectra at some or all of these points as desired. Subroutine GRAPH can be used to present dose rate data in the form shown in Fig. 2.2. A more useful format can be obtained by calling subroutine CONTOR. This causes isodose points in tissue to be plotted by a Calcomp unit, and automatic linear interpolation of intermediate values yields isodose curves as shown in Fig. 2.3. An additional subroutine, AUTOLOAD, has been written which prepares a data input card deck for ZAP from a stored library of β and γ spectra and other physical constants. A report describing the ZAP 3.1 and ZAP 3.2 codes is being prepared.

Data from Bridges et al., Westinghouse Astronuclear Laboratory⁽⁶⁾ have been used in ZAP to calculate the values shown in Figs. 2.1, 2.2, and 2.3. These figures

ORNL-DWG 65-165

```

PELLET RADIUS      .05      COMPOSITION      2
COATING THICKNESS  =0      COMPOSITION      3
AIR COMPOSITION    4      TISSUE COMPOSITION 5
ENERGY STEP, MEV  .100     NO. OF STEPS     25     INITIAL VECTOR NO. 3

```

ANGLE	DISTANCE	DEPTH, CM.	DOSE, RADS.
0	.05	0	1.475E+01
		.05	3.190E+00
		.10	1.183E+00
		.15	5.554E-01
		.20	2.992E-01
		.25	1.765E-01
		.30	1.110E-01
		.35	7.318E-02
		.40	5.005E-02
		.45	3.523E-02
		.50	2.540E-02
		.55	1.867E-02
		.60	1.395E-02
		.65	1.057E-02
		.70	8.105E-03
		.75	6.271E-03
		.80	4.891E-03
		.85	3.841E-03
		.90	3.036E-03
		.95	2.416E-03
		1.00	1.937E-03
		1.05	1.567E-03
		1.10	1.282E-03
		1.15	1.063E-03
		1.20	8.943E-04
		1.25	7.644E-04
		1.30	6.641E-04
		1.35	5.860E-04
		1.40	5.245E-04
		1.45	4.755E-04
		1.50	4.356E-04
		1.55	4.027E-04
		1.60	3.748E-04
		1.65	3.509E-04
		1.70	3.299E-04
		1.75	3.113E-04
		1.80	2.946E-04
		1.85	2.794E-04
		1.90	2.656E-04
		1.95	2.528E-04
		2.00	2.410E-04

Fig. 2.1 Example of ZAP Output Format.

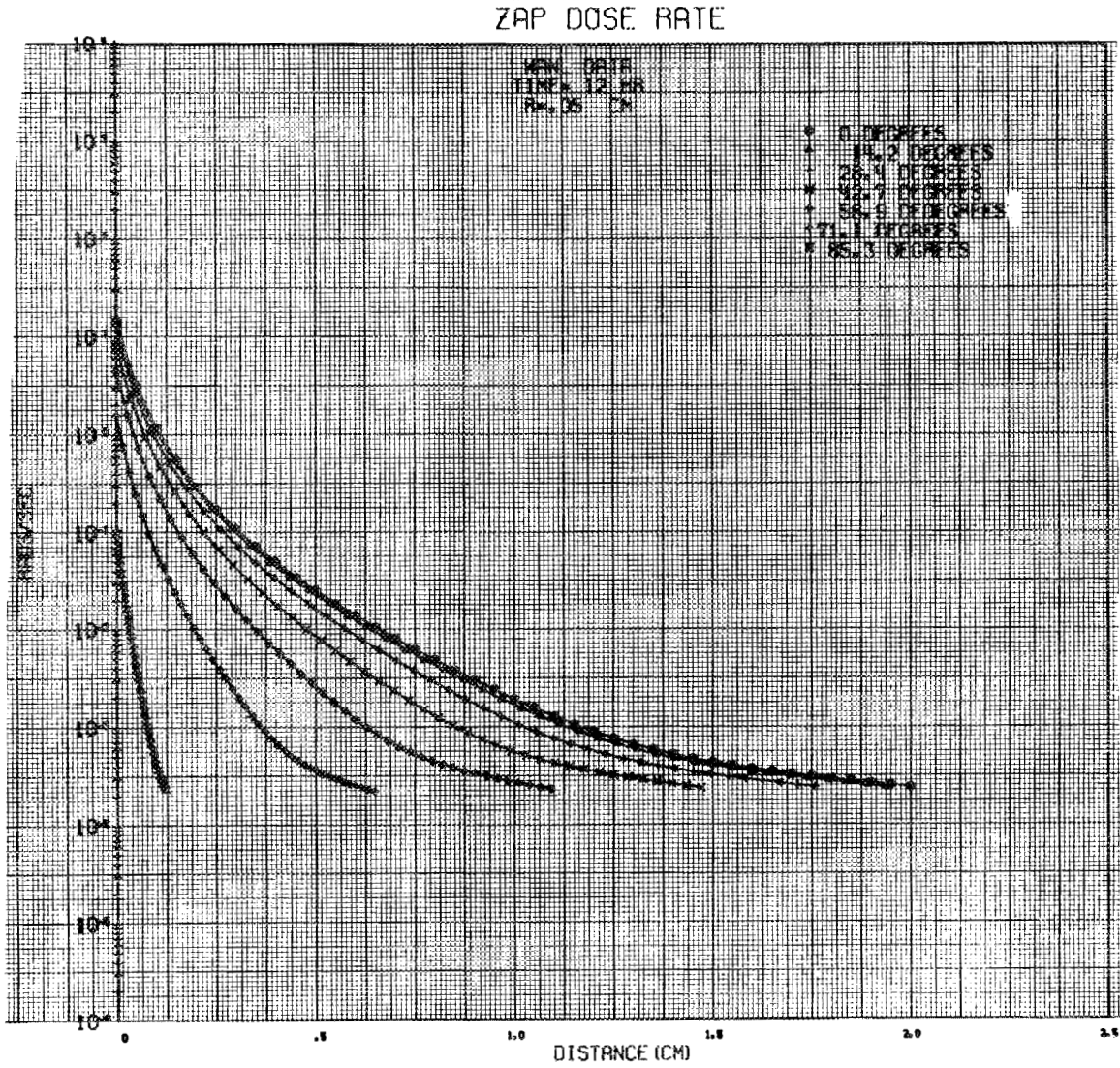


Fig. 2.2 Output of ZAP, Subroutine GRAPH.

ZAP ISODOSE CONTOURS

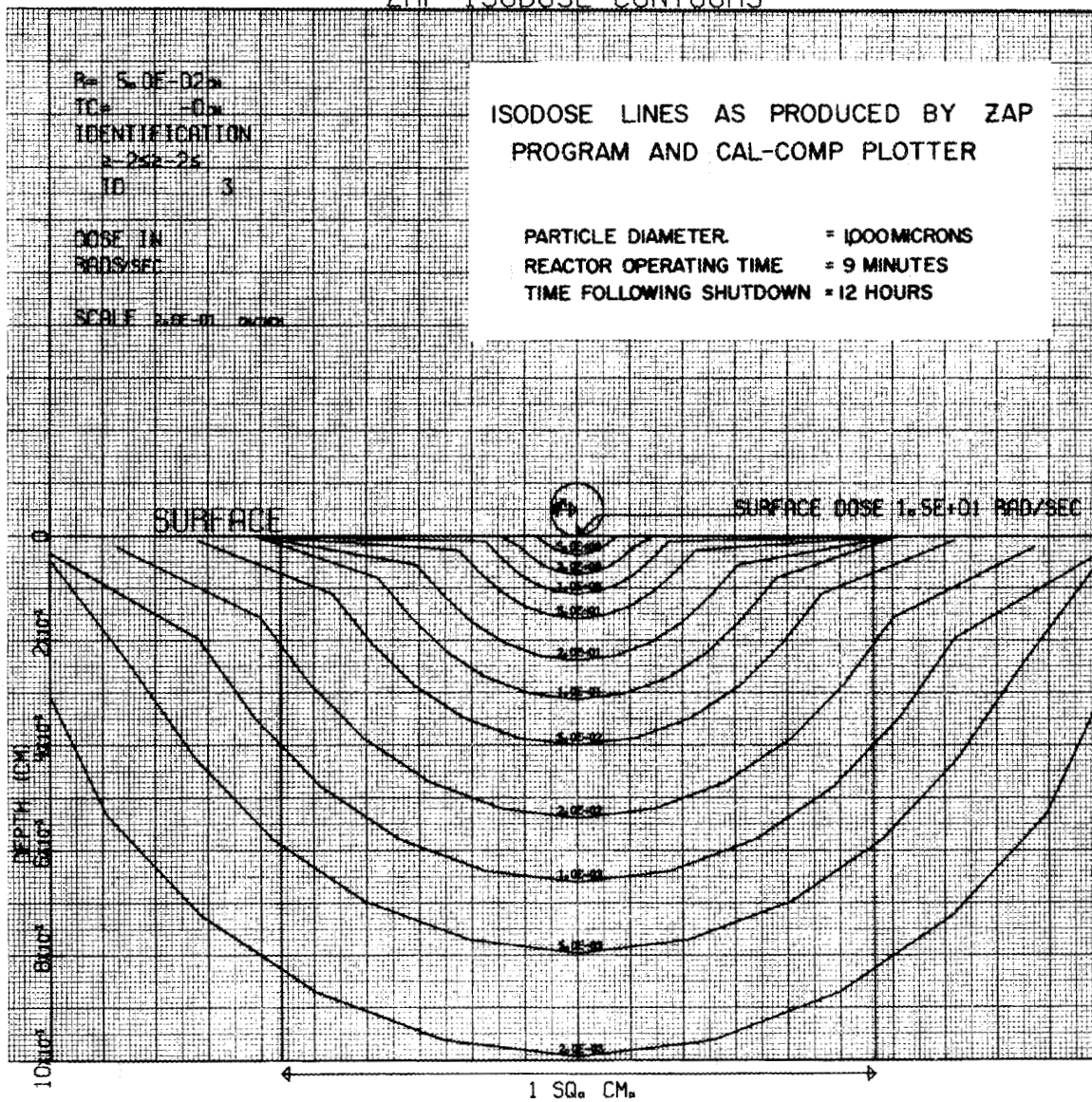


Fig. 2.3 Isodose Lines from ZAP Subroutine CONTOUR

give depth doses from a 1000- μ -diameter particle resulting from destruct of a NERVA engine following a 9-minute power run at 1120 MW. A postoperation decay time of 12 hours yields a fission product inventory for this particle of 2.36 mc of β -activity and 1.93 mc of γ -activity. An ORNL report is being prepared giving depth dose estimates from both 100- and 1000- μ -diameter particles at various times after reactor operation, ranging from 91.8 minutes to 3600 days.

3.0 DOSIMETRY TECHNIQUES

3.1 Introduction

The dosimetry of discrete beta-emitting sources, while difficult at best, nevertheless, is an essential factor in assessing the radiological significance of nuclear reactor debris particles. In this connection two different points of view should be considered. First, it is important to examine the spatial distribution of energy absorbed in tissue and to collate these physical estimates with available radiobiological data, relating effects to comparable absorbed dose. Finally, the expected absorbed doses should be compared to whatever safety control criteria or regulations that may apply to the situation.

The first of these considerations may be met if there are biological data which have been obtained with sources closely similar to those of concern. Otherwise, very careful attention must be given to the distribution of absorbed energy with respect to specific sensitive components of the exposed tissue. Inasmuch as β -particles lose a greater fraction of their energy near the beginning rather than near the end of their range, the dose rate gradient is rather steep in an absorber and is a function of the initial energy. Thus, where there are tissues with degrees of sensitivity to absorbed energy which vary along the range of the β -particle, it makes a great deal of difference just where the energy is deposited. For such tissues, e.g., skin, the use of simplified dose concepts as "range average dose" may be misleading. To provide adequate dose data, simulated and real reactor debris particles are being used in an experimental dosimetry study.

Published recommendations of the International Commission on Radiological Protection (ICRP) do not treat the specific problem of exposure to a single radioactive

particle. However, with regard to exposure of the skin, two significant factors are recognized by ICRP in the derivation of protection criteria.⁽⁷⁾ First, for purposes of calculation the effective depth of the critical skin tissue (basal layer of the epidermis) is assumed to be 7 mg/cm². Furthermore, for the skin the significant area is taken to be one square centimeter in the region receiving the highest dose. Thus, the measurement of dose rate in a 1-cm² dosimeter (Section 3.4) located at the appropriate depth in tissue is of value for comparison with available exposure control criteria.

3.2 Extrapolation Chamber

Construction of an extrapolation chamber, Fig. 3.1, based on Loevinger's most recent model in which a variety of collecting electrodes are available has been completed. The collecting electrodes range in size from 1 mm to 3 cm in diameter. The associated instrumentation has been installed, and preliminary calibrations are being performed. An evaluation of some of the data mentioned in a previous report⁽³⁾ has been made. These data include the measurement of surface dose rate from an ⁸⁹Sr-spiked, 1-cm diameter, simulated fuel sphere (Fig. 3.3) using an extrapolation chamber belonging to R. Loevinger, Stanford Medical Center.

3.3 Film Dosimeters

Some work using film dosimeters has been done in order to assess the uniformity of activity in simulated sources and to get additional information on the variation in beta dose in an irradiated tissue.

In this technique a sheet of film is clamped between two blocks of tissue-equivalent material and the source is positioned on the edge of the film. After exposure the film is developed and the relative blackening, Fig. 3.2, is determined with a recording microdensitometer. By comparison with calibrated films, dose estimates can be made. From these data, isodose lines can be plotted for comparison with computer-derived isodose plots (Fig. 2.3). This technique is now being used to get relative dose estimates and isodensity measurements from small, fuel-debris particles which were obtained from the NRX-A2 Reactor Test (Section 4).

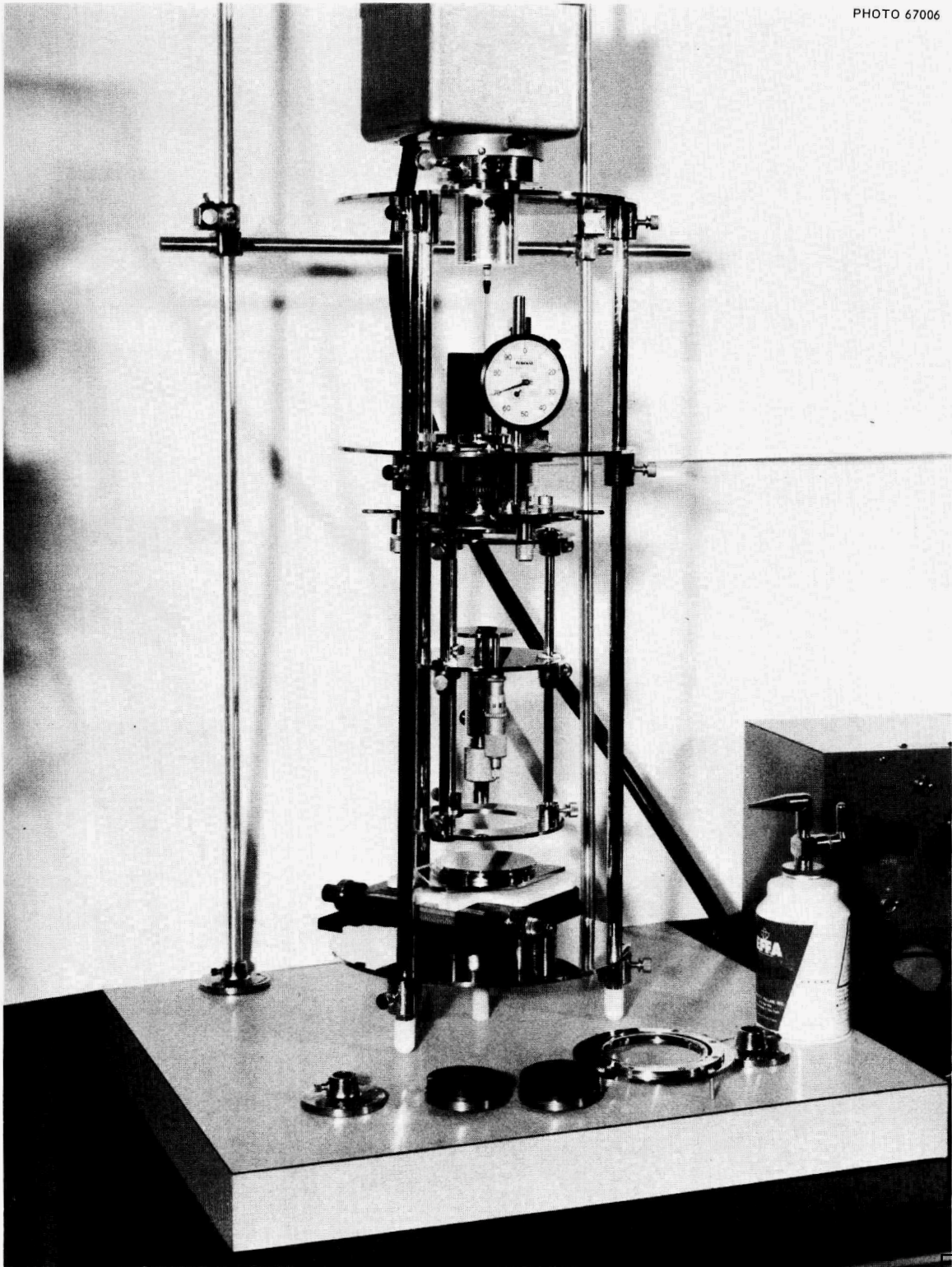


Fig. 3.1 Extrapolation Chamber.

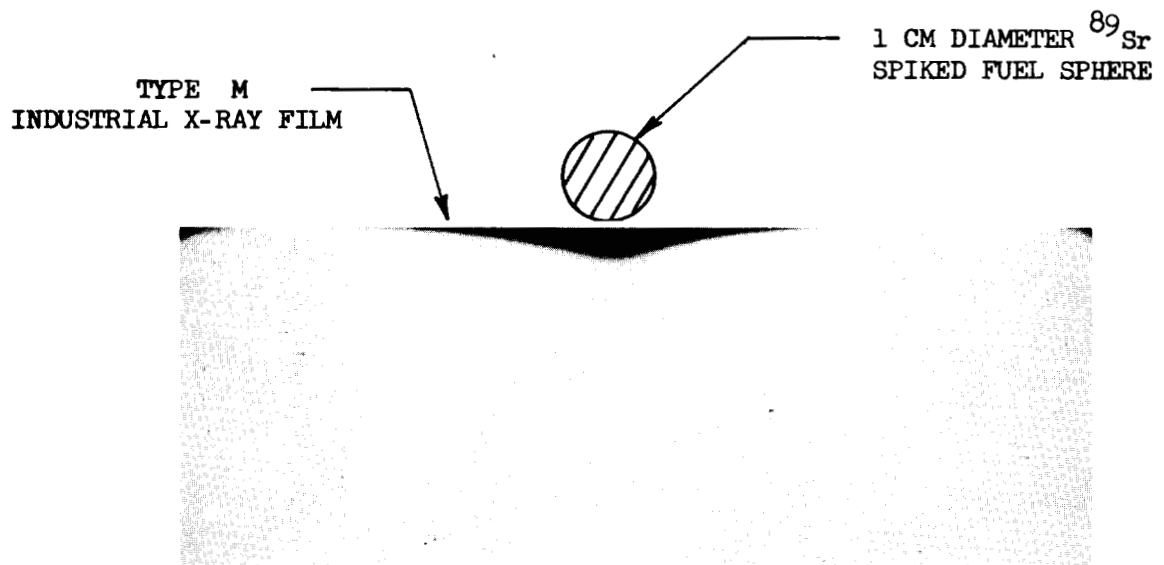


Fig. 3.2 Film Blackening Technique for Establishing Isodose Contours in Tissue (sphere placed on edge of film held between two blocks of plastic).

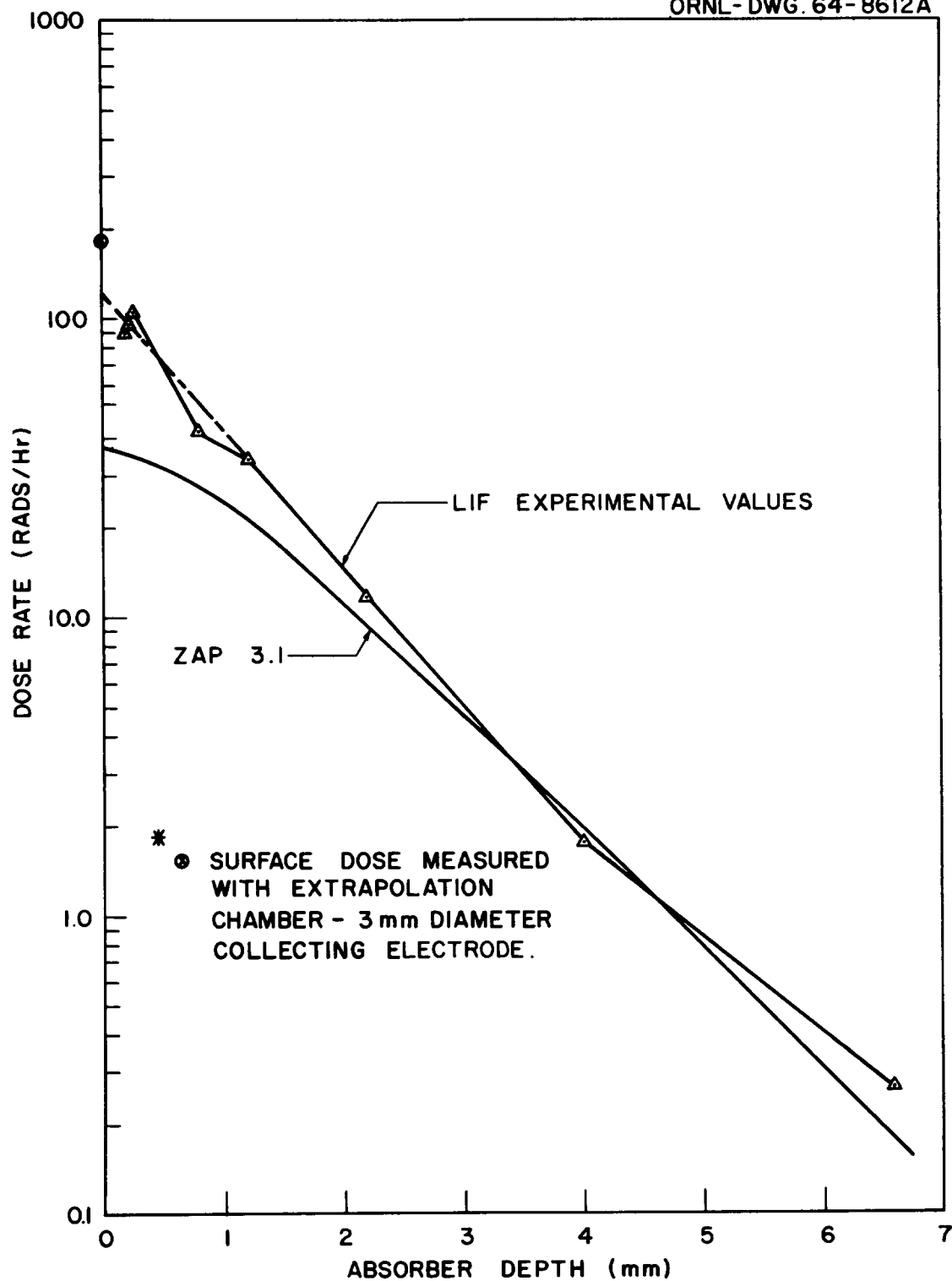


Fig. 3.3 Depth Dose in Tissue From ^{89}Sr Spiked 1 cm Diameter Fuel Sphere (Dose Rate Averaged over 1 cm² Area).

3.4 Lithium Fluoride Dosimetry

Lithium fluoride, depth dose measurements are being made on simulated fuel-debris particles and on debris particles from recent reactor tests. The technique, described in previous reports, ^(2,3) employs a dosimeter reader based on a design of Kenney, et al. ⁽⁸⁾ LiF phosphor is placed in a cavity 5 mils deep and 1 cm² in cross-sectional area, in a polystyrene block. Absorbing layers of polystyrene are placed between the source and the phosphor to the desired depth. The LiF dosimeter reader produces a curve during sample heating, and the glow curve peak is taken as an index of dose. Data are shown in Fig. 3.3 for a 1 cm diameter, ⁸⁹Sr-spiked sphere.

An analog integrator is now being added to the circuitry of the LiF reader in order to record the total area under the glow curve. This technique is expected to yield more reliable results than those obtained from the differential glow curve alone.

LiF thermoluminescent dosimetry will be used as the standard method to measure the dose rate at a depth of 7 mg/cm² averaged over 1 cm² area from each of the simulated fuel debris particles which are now being made. These data, along with the results of other dosimetric measurements, are directly related to an animal-exposure program which is being planned jointly by Battelle Northwest and Oak Ridge National Laboratory.

3.5 β - γ Flux-Spectra Measurements

An anthracene, β -ray spectrometer has been built to measure the emission spectra and emission flux of discrete radioactive sources. This equipment employs a 512-channel, Nuclear Data spectrum analyzer with automatic tape print-out. The measured spectra can be used by the computer program ZAP (Section 2.0), whereas ZAP now uses derived spectra to produce dose estimates. Experimental measurements of the degradation spectra of various sources will be made as a function of depth in tissue, and these will be compared with ZAP calculations of attenuated spectra. A ¹³⁷Cs, thin-film source calibration of the beta-ray spectrometer is shown in Fig. 3.4. A very good resolution is shown for the 624 keV, ¹³⁷Ba, internal conversion electron peak. A number of anthracene crystals are used, varying in size from 1/8 " x 1/8 "

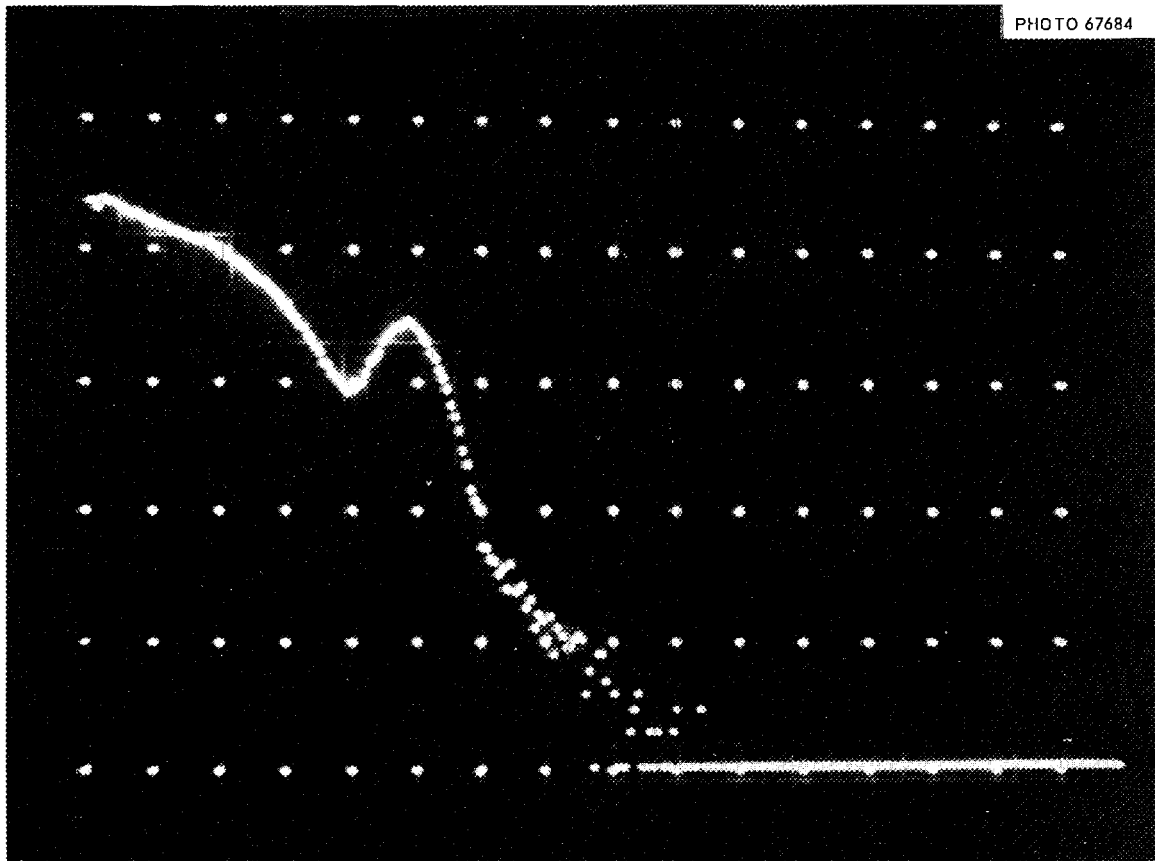


Fig. 3.4 A ^{137}Cs thin-film source calibration of the beta-ray spectrometer.

to 1/2" x 1/2". The crystal is optically coupled to a machined, plastic, light pipe which, in turn, is coupled to a 1" diameter, RCA 6199 photomultiplier.

A beta spectrum has been obtained for a 1 cm diameter fuel sphere spiked with ^{89}Sr and for a debris particle derived from the NRX-A2 test (Section 4.4.2). In addition, the gamma spectra of these sources have been measured using NaI(Tl) crystal spectrometers. These emission spectra may be used in the ZAP computer program for calculating tissue dose, thereby bypassing the various subroutines which are used to produce an estimate of the spectrum.

4.0 EXAMINATION OF REACTOR DEBRIS PARTICLES FROM NRX-A2 TEST

4.1 Introduction

Two particles were received from the September 24, 1964, NRX-A2 reactor test. Assay of the particles was begun immediately to identify the major contributors to dose, to measure β and γ flux-spectra, and to estimate radionuclide content. The equipment for beta spectrum analysis is described in Section 3.0. Personnel of the ORNL in-vivo, gamma spectrometer (IVGS) facility gave much help and advice on the operation of the equipment and also helped by preparing calibration sources of $^{140}\text{Ba-La}$ and $^{95}\text{Zr-Nb}$.

4.2 Particle Description

The reactor debris particles were received in October. Microphotographs, Figs. 4.1 and 4.2, show a considerable difference in shape for the two particles. The smaller particle is approximately spherical and is about 125 μ in diameter, while the larger particle has a marked irregularity in shape and is about 280 μ in diameter.

4.3 Dose Estimates

Lithium-fluoride thermoluminescent dosimeters were used to measure the dose rate at a depth of 15.22 mg/cm^2 which is one thickness of Scotch tape plus 1 mil Saran Wrap and 2 1/2 mils of LiF phosphor. The dosimetry technique is the same as that described in previous reports^(2,3) (Section 3.4). The average dose rate over 1 cm^2 at 15 mg/cm^2 as of November 20, 1964, was 180 mrad/hr for the small particle and 210 mrad/hr for the large particle. A GM survey instrument was used

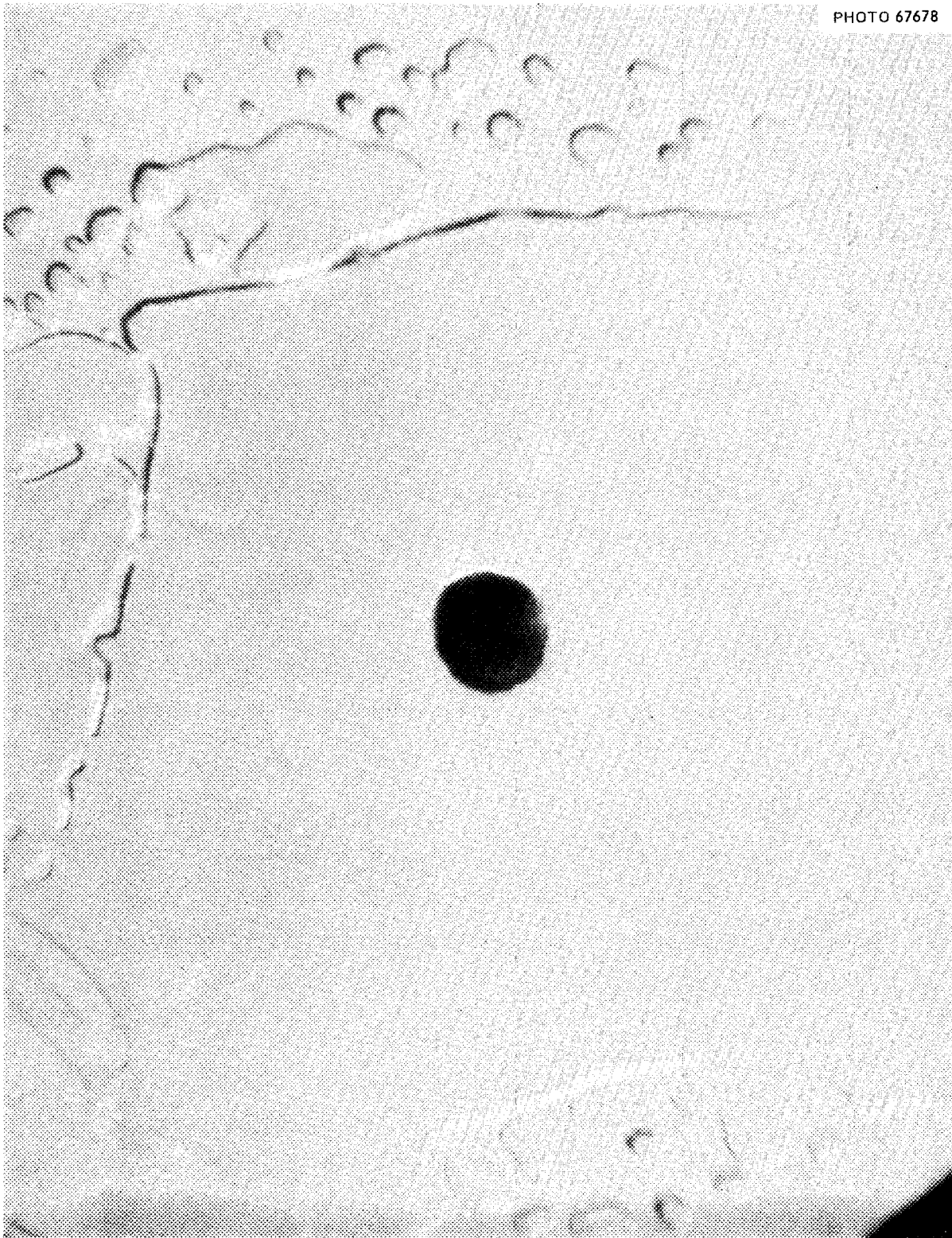


Fig. 4.1 Small Debris Particle, September 24 Test.

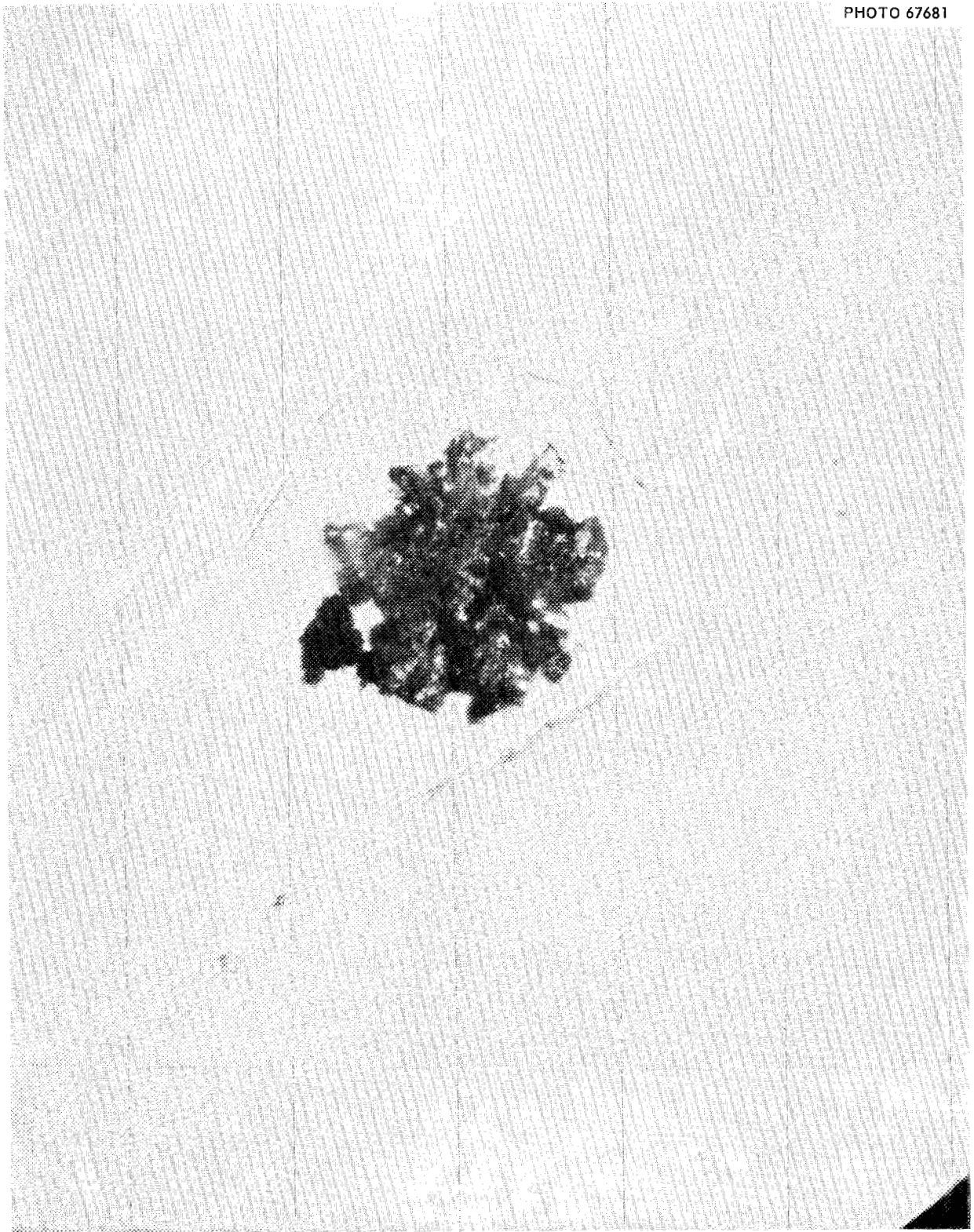


Fig. 4.2 Large Debris Particle, September 24 Test.

to measure the external hand exposure hazard, and dose rates of 22 mrad/hr and 25 mrad/hr were found in air at a distance of approximately 3/4 inch.

4.4 Particle β - γ Spectra

4.4.1 Gamma Spectra

A 4x4-inch, NaI(Tl) crystal housed in a shielded cubicle at the IVGS facility was used to obtain the gamma-ray spectra. Figure 4.3 shows the spectra obtained from the small particle on October 24 (top) and on November 20, 1964 (bottom — data displaced a factor of 10 downward). Each large dot in the 6 horizontal rows represents 16, 8-kev channels starting with channel 0, and the horizontal rows are decade lines with the bottom line representing 1 count per counting period.* Each particle was placed on the crystal axis 6.7 cm distant from the face. The difference spectrum, shown in Fig. 4.4, illustrates the changes in different portions of the gamma-ray spectrum as a result of 24 days radioactive decay. This is almost a pure $^{140}\text{Ba-La}$ spectrum (compare Fig. 4.8).

The gamma spectra obtained on November 20 for both the small particle (top) and the large particle (bottom — displaced a factor of 10 downward) are shown in Fig. 4.5. It is seen that the highest energy photopeak (1.59 Mev- ^{140}La) is approximately the same height for both particles, whereas the next prominent peak of lower energy (0.755 Mev average peak of $^{95}\text{Zr-Nb}$) is significantly lower for the small particle. Thus, despite the fact that the large particle has about 10 times the volume of the small one, the radioactivity content of the two particles is qualitatively the same, with the large particle containing only about 15% more $^{95}\text{Zr-Nb}$ than the other. Presumably, both particles contain only a single fuel bead, and the difference in size represents an additional amount of matrix material in the larger particle.

4.4.2 β -Spectrum

The β -spectrum shown in Fig. 4.6 was obtained from the small particle on October 24, using the equipment described in Section 3.5. These data

* The same scale is used for all spectrum photographs in this report.

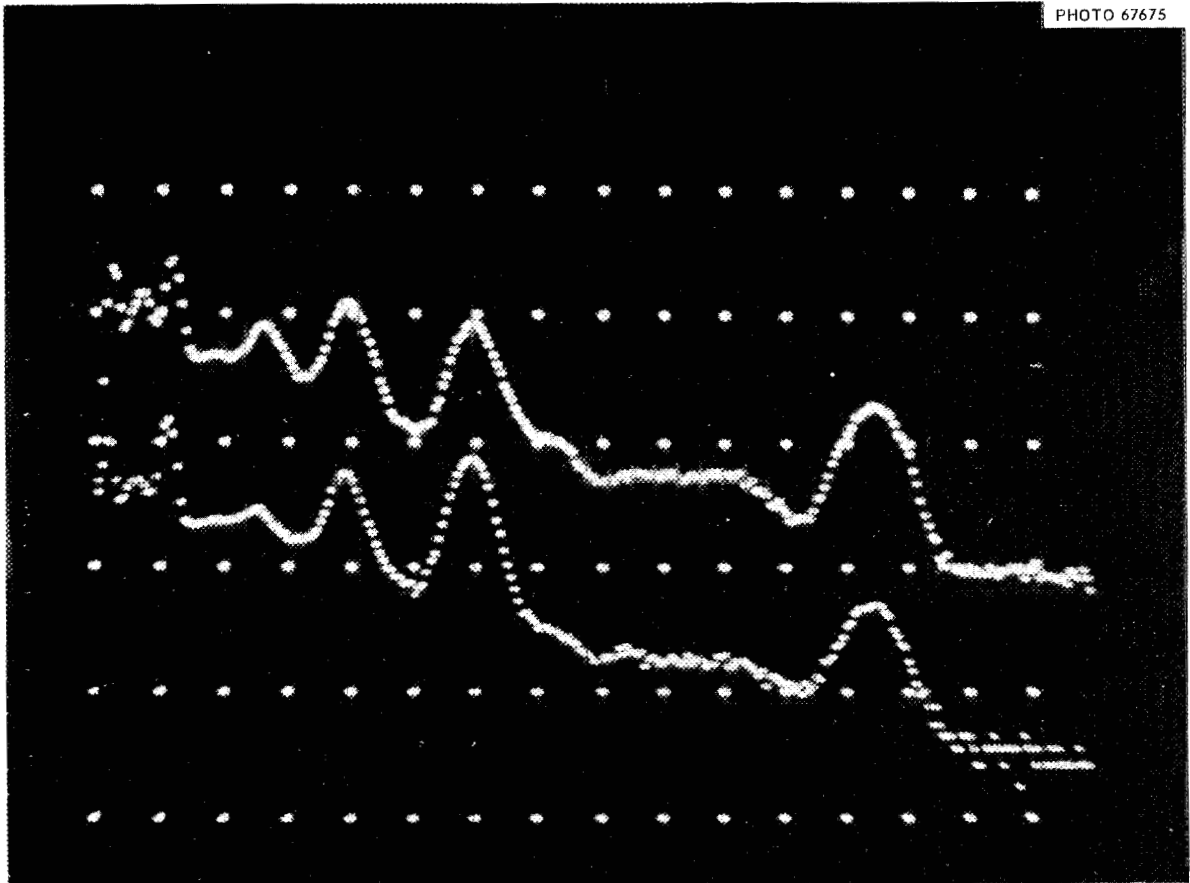


Fig. 4.3 Small Reactor Debris Particle, Comparison Spectra,
27 Days Decay (Nov. 20, 1964).

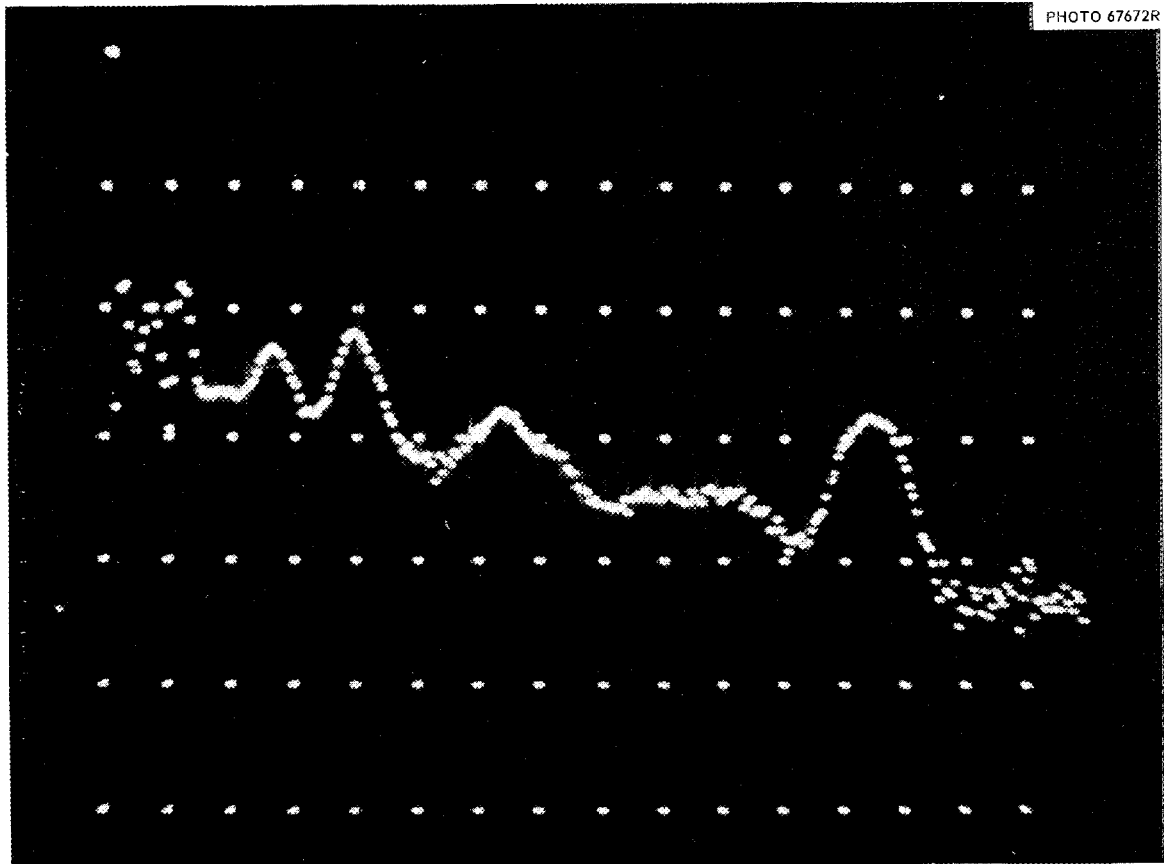


Fig. 4.4 Small Reactor Debris Particle, Difference Spectrum.
(Spectrum Oct. 24) minus (Spectrum Nov. 20).

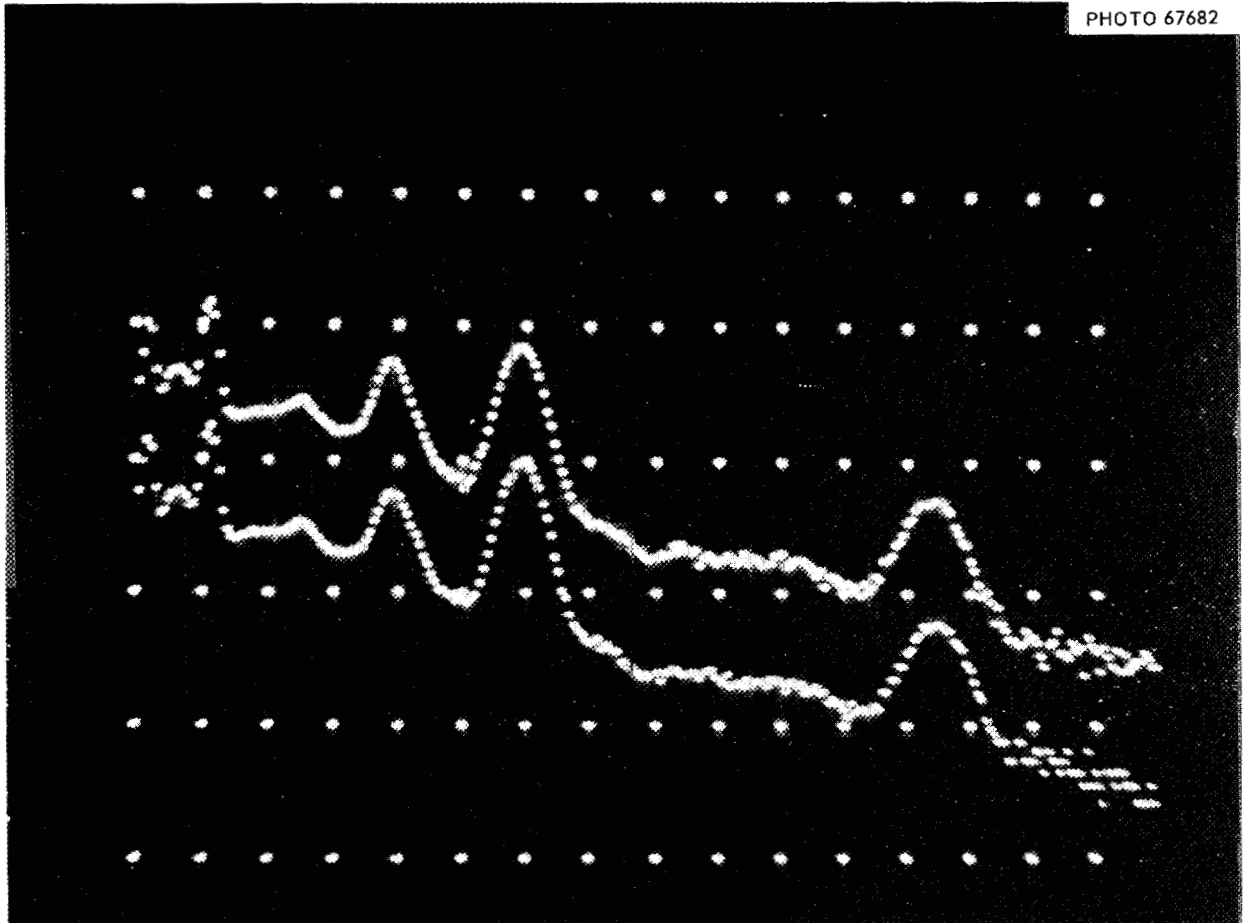


Fig. 4.5 Comparison of Gamma Spectra from Large and Small Debris Particle.

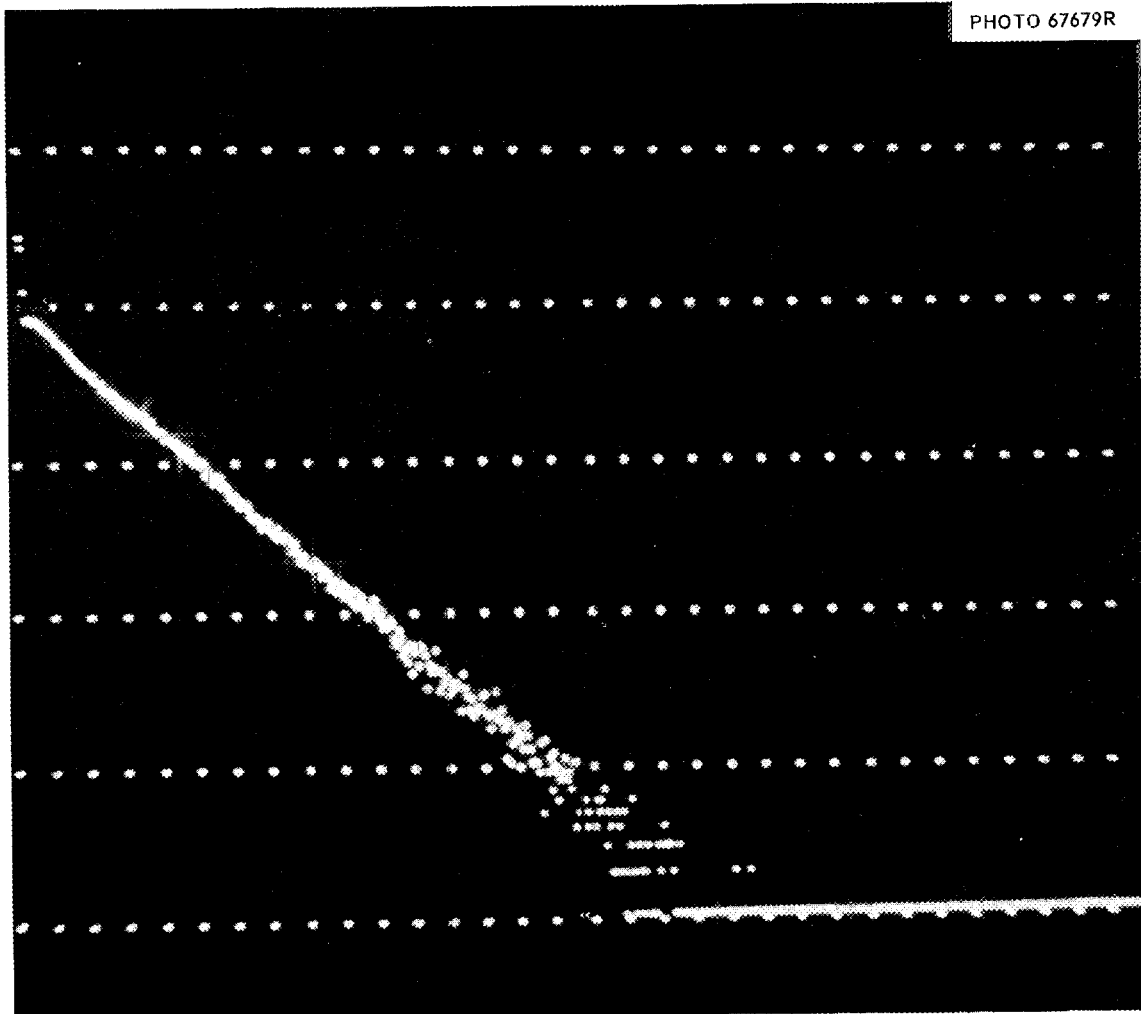


Fig. 4.6 Small Reactor Debris Particle Beta Spectrum, 20 min count, 1/4" x 1/4" Anthracene Crystal, etc.

are replotted (Fig. 4.7) in terms of counts per 8 kev channel for a 20-minute counting time. Assuming 6% geometry, an estimate of the emission flux, in β per second per 8 kev energy interval, can be derived by dividing the count data by 72. The spectrum is represented quite well by a single exponential over nearly 4 orders of magnitude change in intensity. Although the spectrum appears to go to zero at about 2.3 Mev, there is no well-defined end-point energy because of the poor statistics involved. The average energy calculated by integrating under the curve of Fig. 4.7 is 0.4 Mev.

4.5 Radioisotope Content

4.5.1 Estimation of $^{140}\text{Ba-La}$ and of $^{95}\text{Zr-Nb}$

Small point sources were fabricated of $^{140}\text{Ba-La}$ and of $^{95}\text{Zr-Nb}$, and their gamma spectra are shown in Figs. 4.8 and 4.9. These calibration spectra were obtained using a 4"x4" NaI(Tl) crystal and a 512-channel analyzer at an energy response of 8 kev per channel. The amounts of $^{140}\text{Ba-La}$ and of $^{95}\text{Zr-Nb}$ in the debris particle were estimated by comparison with these known spectra.

On October 24, 1964, the small debris particle contained 0.173 μc of $^{140}\text{Ba-La}$ and 0.101 μc of $^{95}\text{Zr-Nb}$. It is estimated that these quantities are known within $\pm 5\%$.

4.5.2 Comparison with Calculated Inventory

Fission product inventory calculations of Kochendorfer⁽⁹⁾ for 0.25×10^7 seconds decay time following a 5-minute operation were adjusted according to the following assumptions:

- (1) 100% of full power corresponds to 1120 MW;
- (2) The NRX-A2 test particles had experienced the equivalent of 6.783 minutes at full power based on the operating history (Sept. 24, 1964)
 - (a) 56% of full power for 6 minutes,
 - (b) 75% of full power for 2.167 minutes,
 - (c) 83% of full power for 2.167 minutes;
- (3) The total mass of the reactor core was 1.2×10^6 grams.

Using the measured quantities of $^{95}\text{Zr-Nb}$ and of $^{140}\text{Ba-La}$, the average specific activities of these isotopes in the total reactor were estimated based

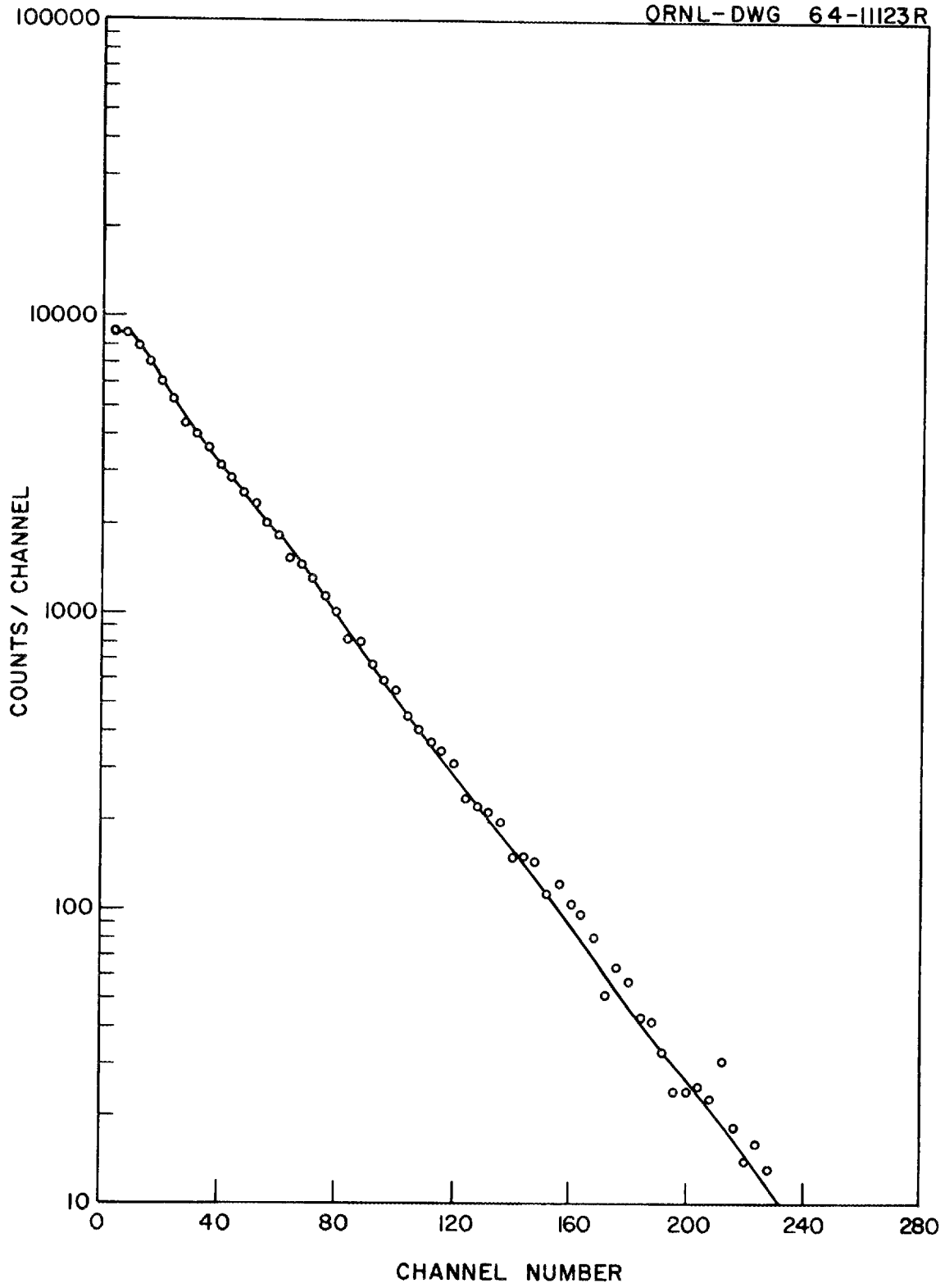


Fig. 4.7 Small Debris Particle, β Spectrum, (20 min. count).

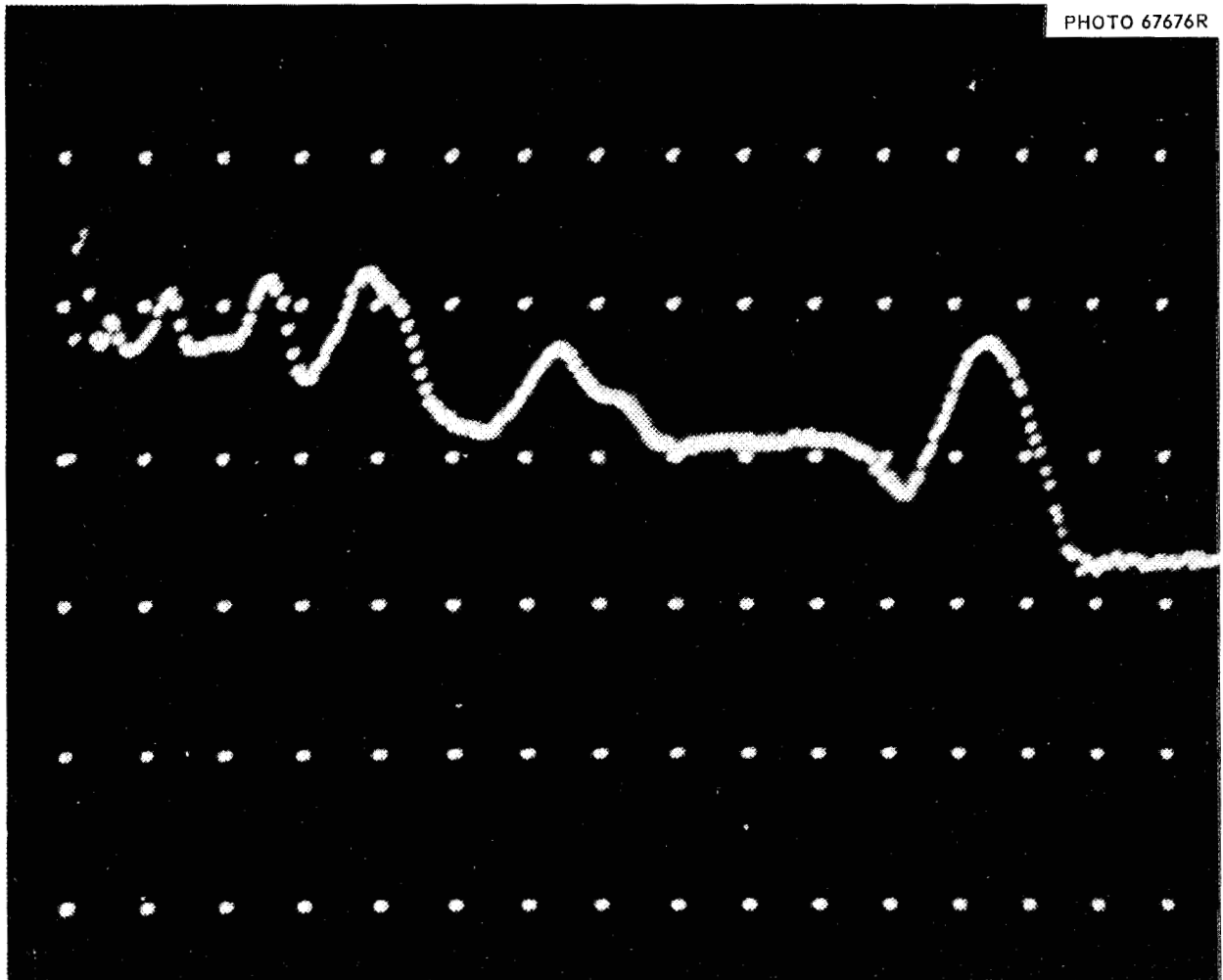


Fig. 4.8 $^{140}\text{Ba-La}$ Calibration Spectrum, etc. (Oct. 24, 1964).

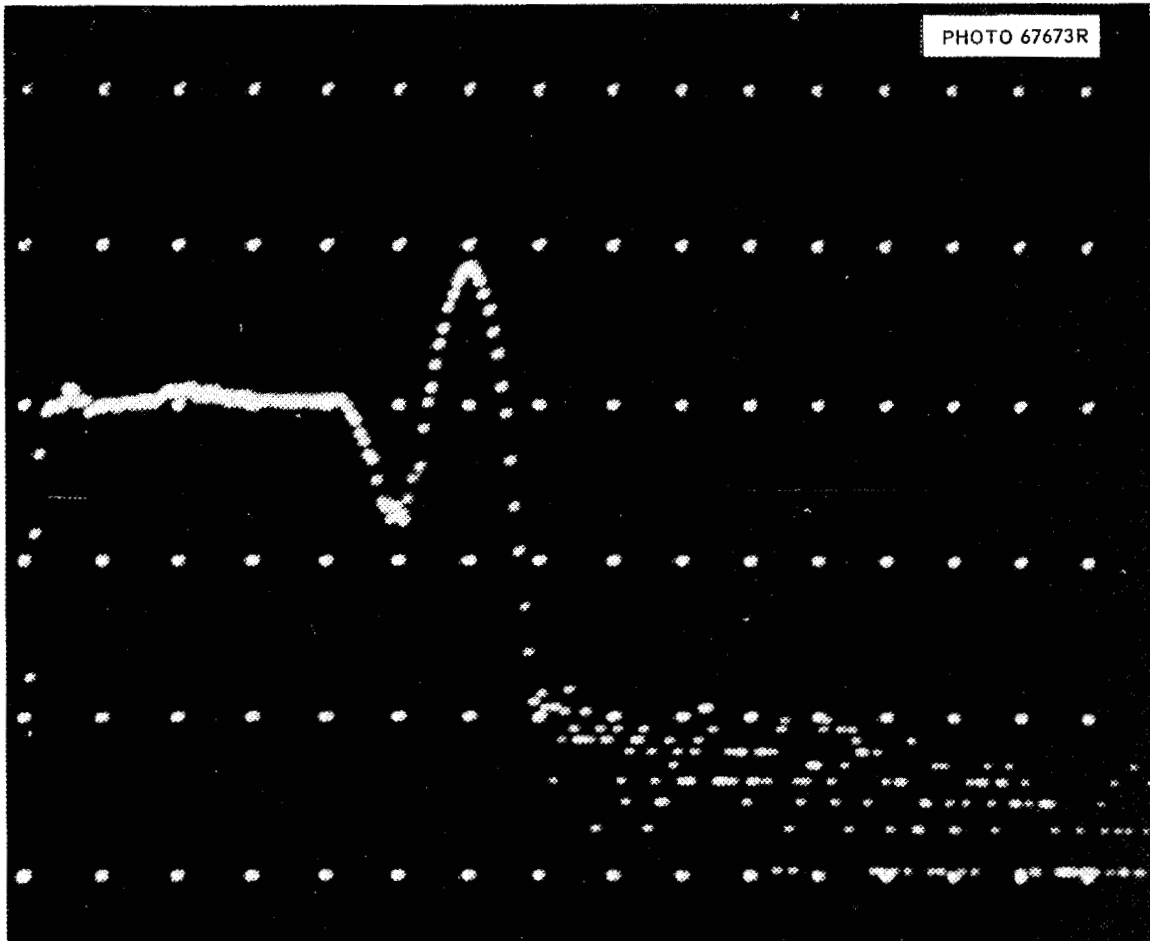


Fig. 4.9 ^{95}Zr -Nb Calibration Spectrum, etc. (Oct. 24, 1964).

on the assumptions that

- (4) The radioactivity in the small debris particle is the average radioactivity in one fuel bead;
- (5) The average fuel bead is 110 μ diameter and 1/27 of the reactor core is composed of such beads;
- (6) Of the $^{95}\text{Zr-Nb}$ and $^{140}\text{Ba-La}$ produced in the bead represented by the small debris particle, none escaped from the particle;
- (7) The average specific gravity of the reactor is 2.0 grams per cubic centimeter.

The estimated specific activities shown in Table 4.1 are affected very greatly by the assumptions used in deriving them. This is especially true in regard to the assumed average bead diameter (110 μ). Thus, no attempt is made to explain the relatively smaller amount of $^{140}\text{Ba-La}$ found in the small debris particle. This appears to be in contrast to the observation (Section 4.4.1) that the small debris particle contains about the same amount of $^{140}\text{Ba-La}$ but somewhat less $^{95}\text{Zr-Nb}$ than the larger particle.

Table 4.1 Estimated Specific Activity of Reactor Debris
30 Days after NRX-A2 Test

	Fission Product Inventory Calculations ^(a)	Based on Small Debris Particle
$^{95}\text{Zr-Nb}$	$2.69 \times 10^{-3} \mu\text{c/gram}$	$2.68 \times 10^{-3} \mu\text{c/gram}$
$^{140}\text{Ba-La}$	$5.43 \times 10^{-3} \mu\text{c/gram}$	$4.57 \times 10^{-3} \mu\text{c/gram}$

^(a)Reference 9

5.0 PRODUCTION OF SPHERICAL PARTICLES

5.1 Carnauba Wax Particles

5.1.1 Particle Description

Fluorescent particles, spherical in shape and ranging in size from 44 μ to 1 mm in diameter, are being made for use in studies of particle transit through

the GI tract (Section 6.0) and of particle retention on human skin (Section 7.0). Particles are spheroidized from a mixture of carnauba wax and Zn-Cd S (Ag) powder which fluoresces strongly when exposed to ultraviolet light. The wax is melted and mixed with the fluorescent material. Rapid cooling is effected by allowing the mixture to solidify in thin layers which precludes the formation of nonuniform concentrations of the fluorescent material by sedimentation.

5.1.2 Spheroidizing Technique

Thin sheets of fluorescent wax are broken and ball milled into small, more or less irregular fragments which are then spheroidized by allowing them to settle through a thermal gradient maintained in a liquid column, Fig. 5.1. Depending on the specific gravity of the particles, the liquid can be chosen so that the settling particles spend sufficient time in the heated portion to be adequately melted. To produce the particles used in the study described in Section 7.0, the column contained a water bath in which the temperature ranged from 96°C at the top to room temperature at the bottom. The top of the column is wrapped with a heating element which maintains the water at a temperature adequate to melt the wax mixture. Small pieces of fluorescent material, introduced into the top of the column, melt and are formed into spheres by surface tension forces. As they settle into cooler portions of the column, the spheres solidify and are collected at the bottom. The particles were found to have a specific gravity of 1.22. Particle size classification is accomplished by washing the particles through a series of sieves. An indication of the relative uniformity of the spheres is given in Fig. 5.2.

5.2 Graphite Particles

5.2.1 Particle Composition

Although the fluorescent wax particles are convenient to use, it is not completely clear what effects the surface composition and specific gravity may have on adhesion to skin. Thus, graphite particles were selected to simulate reactor debris. At present, the particles are being made of HB-type, extra-thin pencil lead and range in size from 300 μ to about 800 μ in diameter. Specific gravity of these particles is 2.0 grams/cm³.

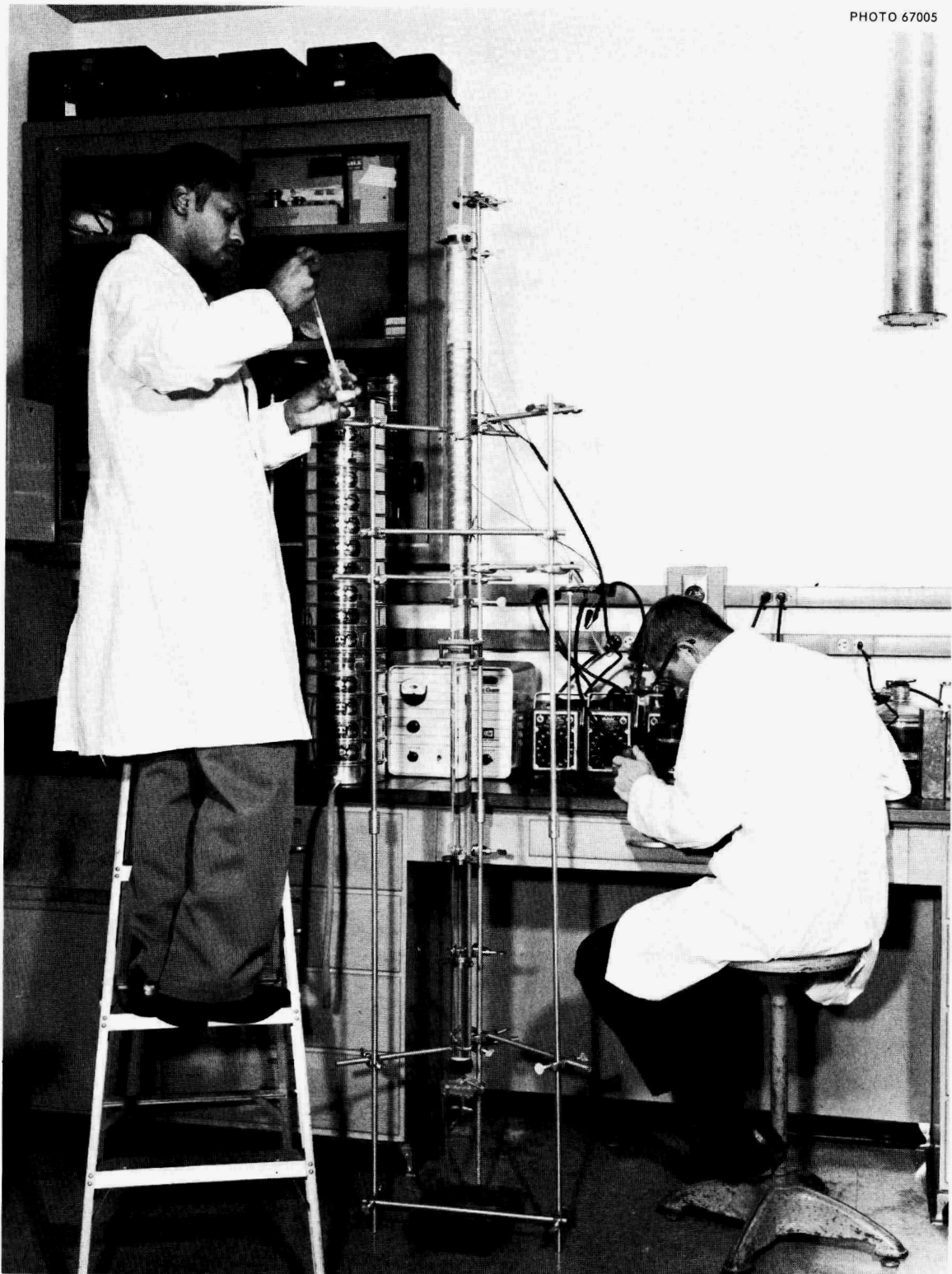


Fig. 5.1 Thermal Column for Spheroidizing Wax Particles.

Fig. 5.2 500-595 μ Diameter Carnauba Wax Particles Containing Zn-CDS (Ag).

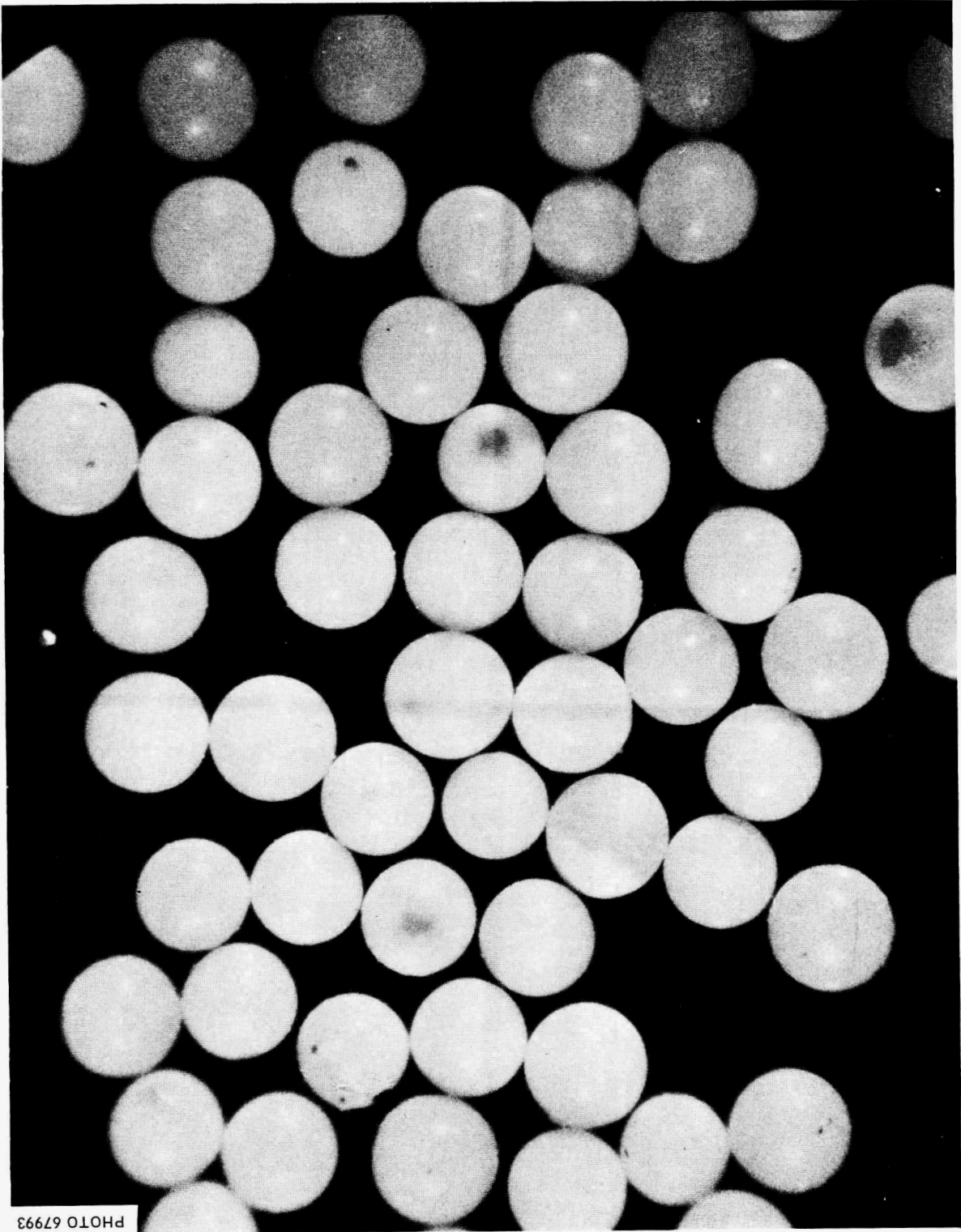


PHOTO 67993

5.2.2 Spheroidizing Technique

Several techniques have been employed to make spheroidal particles out of small cylinders cut from pencil leads, but the most reliable method tried to date is that of hand spheroidizing. In this procedure the particles are rolled with a circular motion between two pieces of abrasive paper, starting with coarse paper and ending with a finer abrasive. Representative particles made by this procedure are shown in Figs. 5.3 and 5.4.

Other techniques of making spherical particles are being explored. An air-operated grinding device, described by Bond,⁽¹⁰⁾ is being fabricated, and tests of the device are anticipated early in January.

6.0 EXPOSURE OF GASTROINTESTINAL TRACT TO "INSOLUBLE" BETA-EMITTERS

6.1 Effects of Radiation on the GI Tract — Literature Review

One of the earlier studies on the effect of internal irradiation on the GI tract was made by Jenkins and McGeorge⁽¹¹⁾ using radium applicators inside the stomach. These and subsequent attempts to reduce gastric acidity in man by this technique are reported by McGeorge.⁽¹²⁾

Pierce⁽¹³⁾ has given the results of the exposure of small numbers of rats to beta and gamma emitters and to mixed fission products introduced by gavage into the animals. Doses in the range 23 to 28 $\mu\text{c/g}$ body weight of fission products caused death in the four rats tested, and in these one perforated stomach ulcer was seen. Seven rats dosed with from 0.4 to 7 $\mu\text{g/g}$ body weight in a single dose showed no effects at one month. Of two rats receiving ^{89}Sr , one died 11 days after a dose of 18 $\mu\text{c/g}$ body weight, and the other was moribund 19 days after receiving 9 $\mu\text{c/g}$ body weight. No histopathological data are given. Five $\mu\text{c/g}$ body weight of ^{91}Y given as a single dose produced "minimal" crypt cell damage. Daily doses of ^{91}Y gave the results shown in Table 6.1. One stomach ulcer was observed in a control rat that had been given daily doses of a saline solution.

With the advent of large-scale radioisotope production, other investigators looked at the effect of nonabsorbable internal emitters on the GI tract. Lisco et al.⁽¹⁴⁾ dosed groups of rats orally with large, single doses (1 to 6 mc) and administered

PHOTO 67991

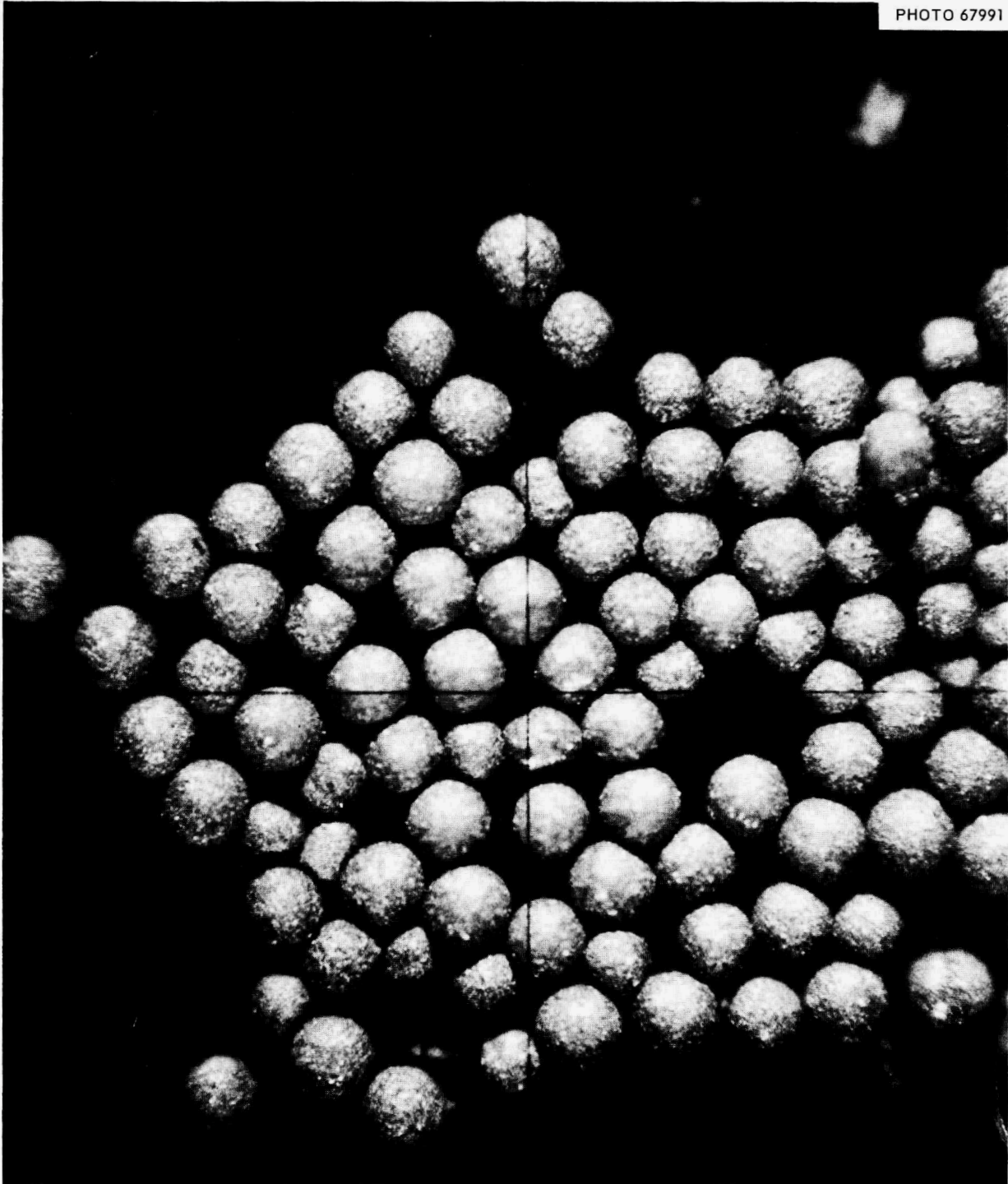


Fig. 5.3 300-400 μ Graphite Particles, Hand Finished.

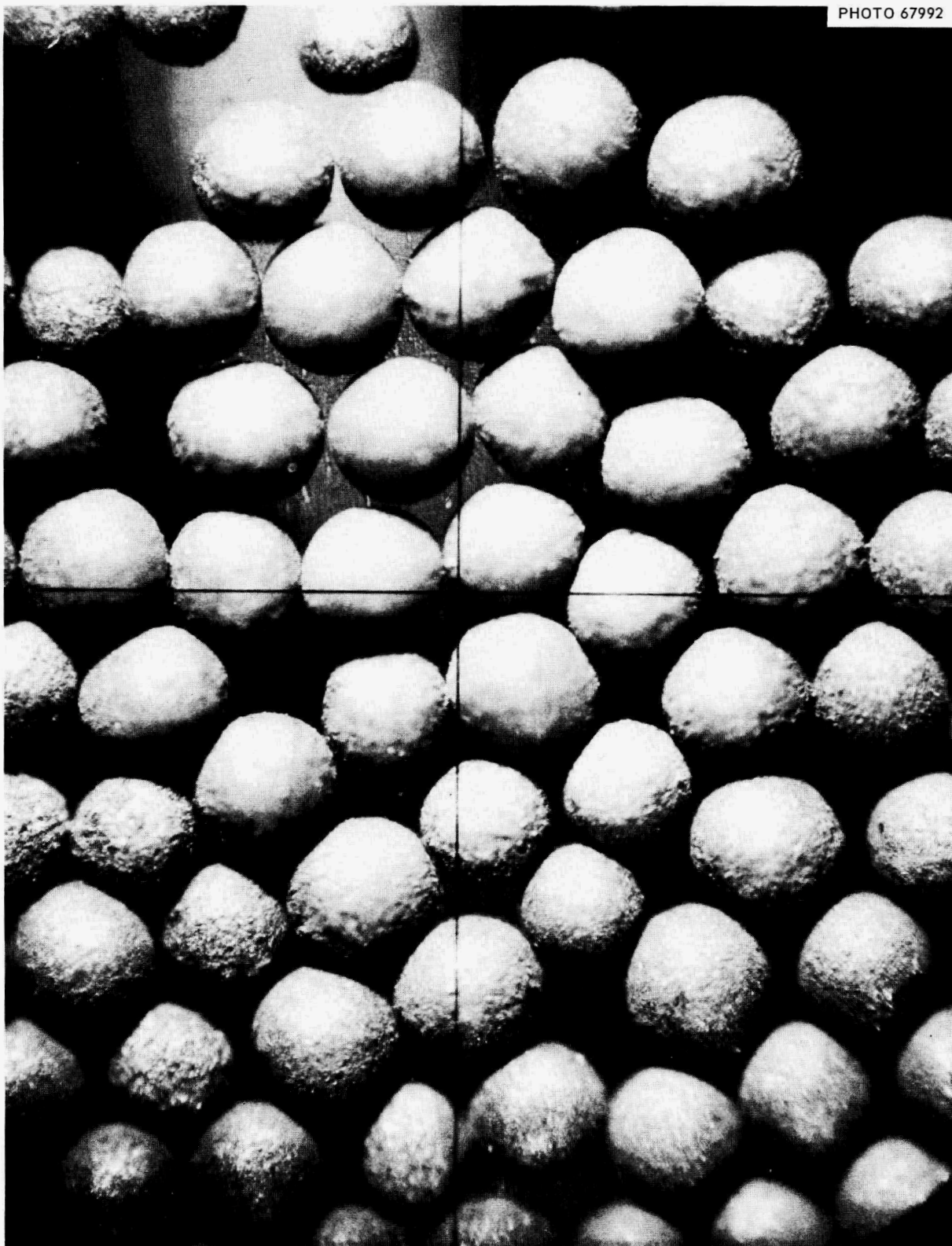


Fig. 5.4 400-700 μ Graphite Particles, Hand Finished.

Table 6.1 Effects of Chronic Ingestion of ^{91}Y in Rats^(a)

$\mu\text{c/g}$ body wt/day	No. of Rats	Duration (months)	Effects
.03	3	6	None
1.0	3	6	Damage in order of increasing severity was seen in: cardiac area of stomach large bowel ileum fundic area of stomach duodenum
2.0	2	3	Similar to 1.0 μc dose; stomach showed more severe damage

^(a)Data reported by Pierce.⁽¹³⁾ The relative insensitivity of the large bowel indicated by these data apparently is in conflict with reports of Lisco,⁽¹⁴⁾ Sullivan,⁽²⁵⁾ and Nold.⁽²⁷⁾

small fractionated doses (.06 to .46 mc) of ^{91}Y to other groups. He observed long-term effects of damage to the colon. Pathological changes varied from superficial ulcerative lesions to adenocarcinoma.

Stomach irradiation of dogs using intracavitary balloons and ^{32}P (refs. 15, 16, 17), ^{131}I (ref. 18), or radioactive noble gases⁽¹⁹⁾ was shown to reduce gastric acidity, usually only temporarily. Doses ranged from 250 rep to 25,000 "equivalent roentgens," and one dog receiving the latter was found to have a mucosal ulcer three months postirradiation.

Fox and Littman⁽²⁰⁾ used solid sources inside balloons, similar to the technique of McGeorge, to test the effect of several individual isotopes on the stomach mucosa of dogs. Aside from the reduction in gastric acidity, the results are summarized in Table 6.2.

Further work by this group indicated that gastrectomy appeared to have prevented death in three of five dogs that received "lethal" doses of radiation to the stomach wall.⁽²¹⁾

Table 6.2 Effect of Radiation on the Gastric Mucosa^(a)

Isotope	No. of Dogs	Dose	Effect
Ra	3	1,500-9,000 mg-hr	Death at highest level in 3 1/2 mos.
¹⁰⁶ Ru-Rh	3	1,600 rbe ^(b)	Chronic gastric ulcer in one
	4	4,800-18,000 rbe ^(b)	All had large gastric ulcers, death within 2 mos
⁹⁰ Sr	3	.75-2.1 curie hrs	None
	5	3-6 curie hrs	Chronic gastric ulcer
	2	12 curie hrs	Chronic ulcer; death within 1.5 mos

(a) Data reported by Fox and Littman.⁽²⁰⁾

(b) Author's units: rbe = Roentgen beta equivalents (approximately equals rad)

Rothe and Tuttle⁽²²⁾ used an essentially insoluble compound, CrPO₄ labeled with ³²P, in a study using rats that yielded information both on transit time through portions of the GI tract and on clinical and histopathological changes. A portion of their results dealing with the stomach is summarized in Table 6.3. By an extrapolation, which the authors agree is not normally permissible, they estimate that man would incur only a minor risk of GI-tract damage by the daily ingestion of 445 µc of insoluble beta-emitting fission products over a 10-day exposure period. Assumptions and equations used in calculating the radiation dose to the gut wall were taken from a paper by Thompson and Hollis.⁽²³⁾ The latter group had used tracer amounts of ¹⁰⁶Ru to derive estimates of transit times and doses to the GI tract of rats from beta-emitting isotopes.

A similarity of effect of x-irradiation and internal beta irradiation of the GI tract on the depression of serum albumin of rats was noted by Palmer and Sullivan.⁽²⁴⁾

Table 6.3 Effects of Chronic ^{32}P Ingestion on Rat Stomach^(a)

μc of ^{32}P /day	No. of Days	No. of Rats	Total Dose (rep)	Effect on Stomach
100	10	4	600	None
	20	3	1,200	None
	30	2	1,800	None
200	5		475	None
	10		950	Minimal
400	5	9	1,300	Abnormal epithelial cells
	10	6	2,600	Degeneration and death of epithelial cells

^(a)Data of Rothe and Tuttle⁽²²⁾ using $\text{Cr}^{32}\text{PO}_4$.

Oral doses of ^{91}Y in the range of 10 to 50 mc/kg body weight gave an LD 50/30 for rats of about 17 mc/kg in a study by Sullivan et al.⁽²⁵⁾ Hematological changes differing slightly from those seen in whole body exposures were evaluated. At all levels the greatest damage was to the large intestine, presumably due to the longer retention time of the radioactivity in that portion of the gut. Changes seen were comparable to those following x-irradiation.⁽²⁶⁾

Observations by Nold et al. on transit time and biological effect of ^{90}Y fed to dogs and goats give further evidence for the selection of cecum and colon as the more critical segments of the GI tract.⁽²⁷⁾ This conclusion holds true when dealing with insoluble beta emitters homogeneously mixed with intestinal contents and with the mass moving through the tract on a known, normal time schedule.

That these GI-tract-transit-time schedules can be quite variable in man was shown by Hayes et al.⁽²⁸⁾ using ^{140}La as a tracer. In this report, dose estimates

to the lower large intestine from the ingestion of nonabsorbed beta activity are made as a function of transit time.

Recent work by Bell^(29,30) on the radiotoxicity of $^{144}\text{Ce-Pr}$ in sheep has shown that some individual animals are remarkably resistant to the lethal effects of massive oral doses of this material. Of 12 sheep fed 1.2 curies over a 60-day period, 4 showed no clinical effects. Necropsies on 6 animals that died showed maximum injury to the omasum and abomasum. This was partially attributable to the lower moisture content of the material as it passed through these segments and the consequent more intimate contact of gut wall and radioactivity.⁽³¹⁾

Daily doses of from 91 to 410 μc of ^{90}Y per rat over a 60-day period via drinking water resulted in a surprisingly high incidence of oral carcinomas and uterine adenocarcinomas as reported by Sullivan et al.⁽³²⁾ Only two intestinal tumors were found over the subsequent lifetime of the experimental animals. Eve⁽³³⁾ gives a brief discussion of this work and the work of others, concluding that beta irradiation is an unlikely carcinogenic agent in the large intestine.

Energetic beta emitters in small animals can insult tissue and organs distant from the source. The production of uterine adenocarcinomas has been mentioned above. Somatic radiation damage to rat embryos from the ingestion of single doses of 0.5 or 1.0 mc of $^{144}\text{Ce-Pr}$ resulting in high resorption rates and physical defects in the young was reported by McFee.⁽³⁴⁾ Hulse⁽³⁵⁾ has produced lethal damage to the intestine of mice using external $^{90}\text{Sr-Y}$ irradiation.

6.2 Transit of Insoluble Particles through the GI Tract

It should be noted that the great majority of the literature surveyed in Section 6.1 deal with the hazards from nonabsorbable radionuclides uniformly mixed with the contents of the GI tract. Radiation dose rate to tissue was calculated from assumed or measured residence times of the source in each segment of the tract. An assumption of uniformity of distribution of activity in the lumen gave an assumed uniformity of radiation to the walls. Thus the dosing technique, where the activity was given as a solution or as a suspension of very small particulates, greatly simplified the comparison of radiobiological effect with radiation delivered. Hazardous levels

of insoluble beta emitters can be extrapolated from such data only if the radioactivity is finely divided and thoroughly mixed with other ingesta, the average transit times through segments of the GI tract are well known, and the resulting irradiation of the gut does not alter these "normal" transit times.

If the activity should be contained in a single insoluble particle, new questions must be answered. One of the more important ones deals with the residence time of the particle in each division of the GI tract. A literature search has begun on the passage of inert material through the GI tract of man, and preliminary indications are that transit times of such material are more variable than that of ordinary food-stuffs. Bizzell *et al.*⁽³⁶⁾ dosed one rat with a bakelite powder labeled with 54 μC of ^{32}P and reported that only 50% had been eliminated by 36 hours. A pilot study by Fish *et al.*⁽³⁾ revealed significant amounts of radioactivity remaining in the stomach of a pig one week following an oral dose of ^{90}Sr -Y titanate in powdered form. This was due in part to the entrapment of particles by areas of ulcerated mucosa.

6.3 Retention of Small Particles in the GI Tract and Their Proximity to the Wall During Transit

In order to estimate dose delivered to the wall of the GI tract, it is necessary to obtain information on the pattern of movement of small particles as they traverse the alimentary canal. A technique based on a suggestion by Decker and Goldman⁽³⁷⁾ for determining the proximity of particles to the gut wall is being evaluated. Spherical particles of variable composition and density and containing a fluorescent tracer are given to experimental animals via food, drinking water, or gavage. Phosphors of various colors may be used to tag particles given at different times or of different physical characteristics. At some time the animal is killed and the viscera immersed immediately in isopentane at liquid-nitrogen temperatures. Thin traverse sections of the gut are examined microscopically under ultraviolet light, and the position of the particles with respect to the wall is noted.

One rat has been fed spherical particles of caruaba wax containing ZnS-CdS (see Section 5.1). Particle diameters ranged from 149 to 177 μ in diameter and were placed in the drinking water 30 hours before necropsy. Two-millimeter-thick

sections were made of the entire length of the tract, and counts were made of the particles within an arbitrary distance of the wall, Table 6.1. Figure 6.1 shows a section of the duodenum with one particle about 500 μ away from the nearest mucosal surface.

Table 6.1 Fluorescent Wax Particles^(a) in the GI Tract of a Rat

Organ	Particles within 500 μ of Wall		Total Particles in Organ	
	Number	% of Total in Organ	Number	% of Total in GI Tract
Stomach	48	63	76	19
Duodenum	1	33	3	< 1
Jejunum-Ileum	5	56	9	2
Cecum	64	47	137	35
Ascending and Traverse Colon	29	51	57	14
Descending Colon	55	48	114	29
Total	202	51	396	-

^(a) Specific gravity = 1.22 g/cm³

Direct counting by eye is tedious, but because of the difficulty in matching UV light sources, film spectral response and fluorescent spectra, photography has not yet been a useful tool in this procedure. Nevertheless, the data are needed to aid in evaluating the potential hazard of an ingested single radioactive particle. Therefore, it is planned to repeat this technique with a larger number of animals to provide statistically valid estimates of transit times and of spatial relationships.

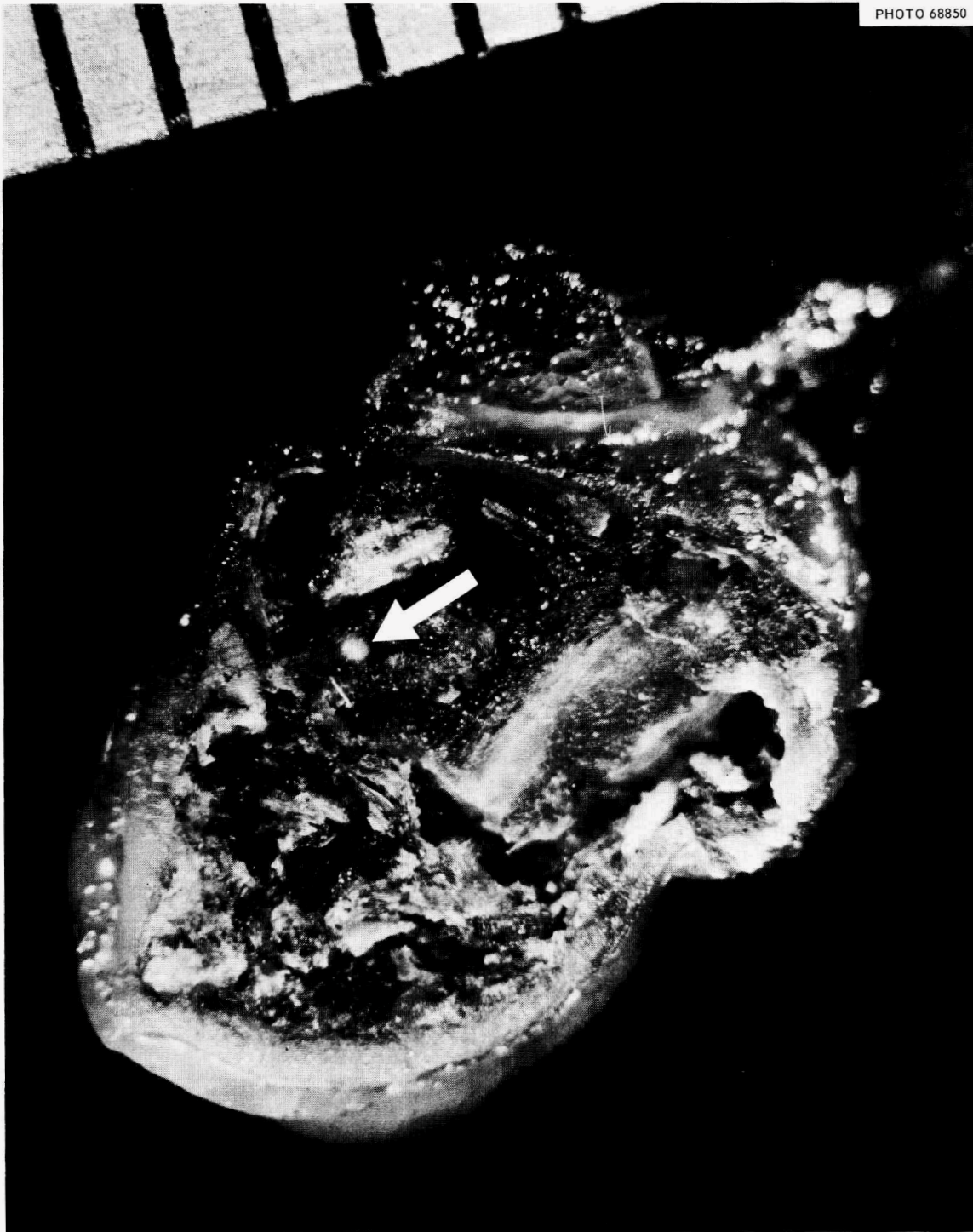


Fig. 6.1 Fluorescent Wax Particle (arrow) in a Transverse Section of a Rat Duodenum.

7.0 EXPOSURE OF SKIN TO DISCRETE PARTICLE SOURCES

7.1 Introduction

In addition to the dependence on the usual source parameters, surface and tissue depth dose is also a function of particle sticking probability and particle retention time. An investigation of the retention of small particles on skin is now under way. A study of the retention of fluorescent wax particles on skin has been completed, and some of the data are summarized in this report.

7.2 Initial Deposition of Particles Falling on the Skin

No formal study of this subject has been made, although an experiment is planned to yield the necessary information. Preliminary inquiry suggests an initial retention of 10 to 20% for 1-mm particles and approximately 100% for particles smaller than about 200- μ diameter.

7.3 Retention of Particles on Human Skin

7.3.1 Introduction

A pilot study of particle retention on human skin was made using particles composed of a thermosetting plastic (Turtox) mixed with Zn-CdS (Ag) powder. Except for the composition and the fact that the particles were more angular than rounded, the techniques used were the same as in the work with fluorescent wax particles discussed below (7.3.2). The results with the angular plastic particles were essentially the same as observed when the wax spheres were used. The differences in the average retention times for the two materials were less than differences seen between individuals with the same type particles. These and other observations suggest that the major parameters are moisture level on the skin (and other liquids, e.g., oiliness), weight of the particle, degree of physical activity, and, probably somewhat less important, the geometry and composition of the particle. These questions will be explored more thoroughly in additional, more detailed studies using graphite (specific gravity 2.0) and other particles.

7.3.2 Retention of Wax Particles on Skin

Carnauba wax was chosen because it melts at a temperature between 86 and 90°C; thus it can be spheroidized in water yet remains hard at normal human

body temperature (37°C). The fluorescent powder Zn-CdS(Ag) was selected because of its high efficiency and also because its color (brilliant yellow-orange) contrasts well with the background of fluorescent material found on the forearms of local volunteers. Normal fluorescent background, in our experience, has been widespread and fluoresces a medium-bright, light-blue, due mainly to the presence of detergents in lint collected on the skin. It is to be expected that background may depend upon many factors of local geology as well as of local customs; accordingly, the choice of a fluorescent tracer should be verified before using the technique in a new geographical area.

Wax spheres, produced by the procedure outlined in Section 5, were separated into limited size ranges by wet sieving. Six sizes were used in this study: 50 to 74 μ ; 74 to 88 μ ; 125 to 149 μ ; 250 to 297 μ ; 500 to 595 μ ; and 1-mm diameter. The particles were dropped from a height of about 5 centimeters onto the flexor and the extensor surfaces of the forearms of human volunteers. From three to six subjects participated in each run which consisted of a set of determinations of retention time for one particle size. A minimum of 60 particles were used on each subject (1 mm), and usually there were more than 100 per subject.

Detailed results of the study will be published as a separate report. In the interim, the following summary of the major findings may suffice for estimating retention time as a basis for radiation dose calculations.

Graphs of particle retention as a function of time for individual subjects vary widely. Nevertheless, the general trends with particle size (mass) are about the same, that is, for two subjects having grossly different fractions retained after the initial half-hour, the adhering particles are lost at approximately the same rate. It appears that there are two components of retention. One component consists of particles relatively loosely held in comparatively dry regions of the skin; these are the easiest to remove, and the rate of removal is related to particle mass and to degree of movement (acceleration). The second component may consist of particles more tightly bound in moist or oily areas of the skin; removal of these particles may require greater force than normal accelerations afford, thus the probability of a direct hit of the particle and removal by some brushing or abrasive action may control the

rate of loss from skin. Since this is a study of natural attrition of adherent particles, deliberate decontamination by washing was not included in the schedule; however, it was observed that normal bathing is essentially 100% effective for removing particles in the size range $> 50 \mu$ from skin.

The retention of particles on skin is seen to decrease with time and follows a two-component exponential function. Retention of smaller particles is adequately described by a single exponential function of time,

$$R = A e^{-t/T} \quad (1)$$

where

A = the fraction sticking initially,

T = average lifetime of a particle on the skin (equals $T_{\frac{1}{2}} \div 0.693$ where $T_{\frac{1}{2}}$ is the half-life for retention),

R = the fraction remaining at time t .

Retention of larger particles may be described by

$$R = B e^{-t/T_B} + C e^{-t/T_C} \quad (2)$$

where

B = the fraction retained with the average lifetime, T_B ;

C = the fraction with average lifetime, T_C ;

R = the fraction remaining at time t .

The average lifetime is determined by integrating $R dt$ from 0 to infinity; thus (from (2))

$$T = \int_0^{\infty} R dt = B T_B + C T_C \quad (3)$$

which is just the weighted average retention time for the given size particle. Figure 7.1 presents the average retention time of wax particles on human skin for the six particle size groups noted above. The observed average life of 1-mm particles on skin seems rather high and will be rechecked. Pending future studies, however, the assumption of the average retention times shown in Fig. 7.1 should not lead to excessive error.

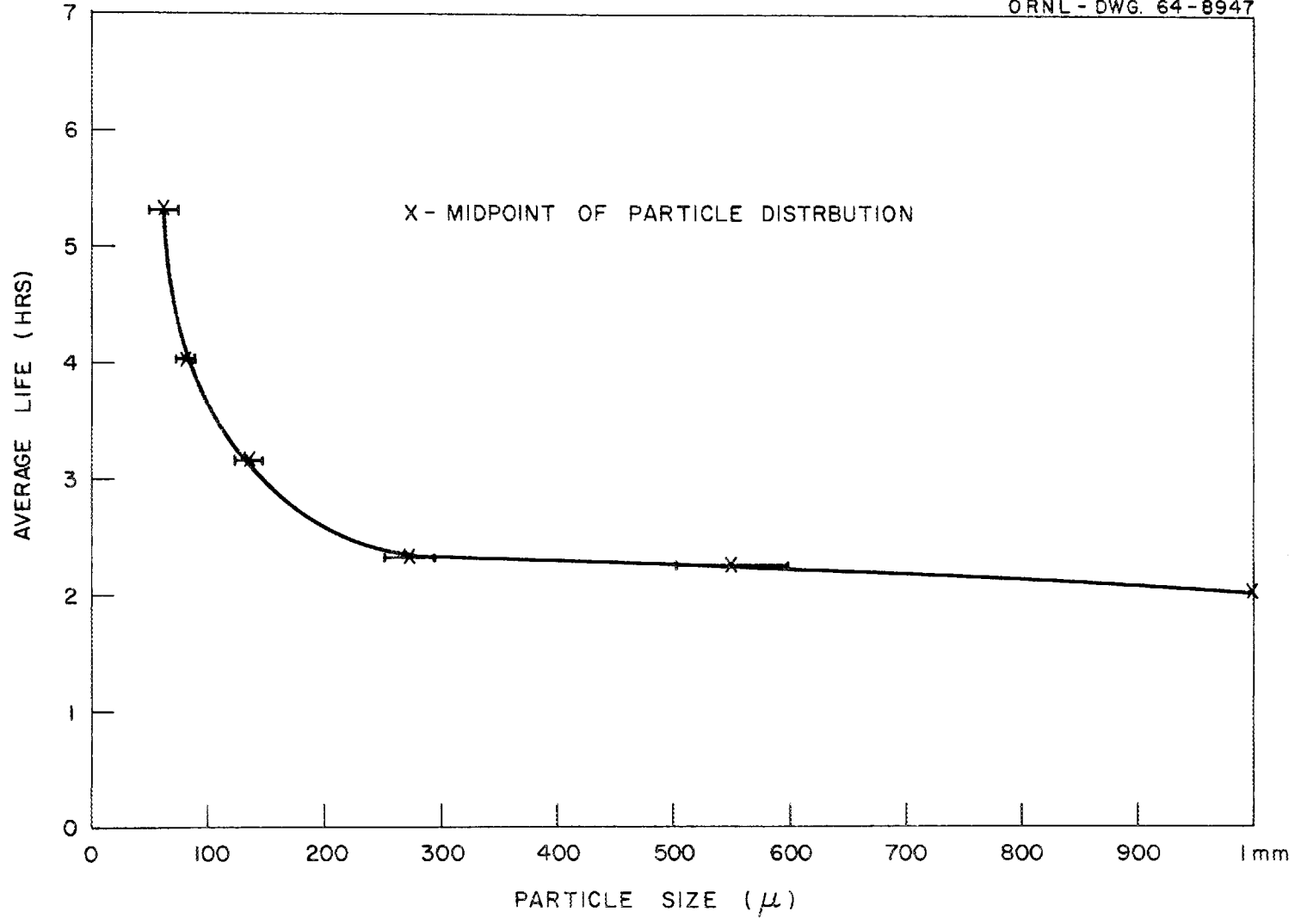


Fig. 7.1 Particle Retention on Skin.

8.0 SOLUBILITY

Particles of reactor fuel containing the proper loading of enriched uranium⁽³⁾ have been obtained from the Y-12 Chemical Engineering Development Department. These fueled spheres will be irradiated in a reactor at relatively low neutron-flux levels for times corresponding to possible operating times of a nuclear rocket reactor. After irradiation the particles will be used to determine the extent to which radio-nuclides are leached out in simulated body fluids.^(1,3) Some of this series of particles can be used to study in vivo solubility in animals and, possibly, for effects studies, depending upon the specific activity of the particles. No solubility work has been done during this report period pending availability of facilities for handling irradiated fuel.

9.0 TRIPS AND MEETINGS

<u>Date (1964)</u>	<u>Location and Purpose</u>	<u>Traveler*</u>
Aug. 1	Orlando, Fla. Attend meeting of executive council of American Association for Contamination Control	BRF
Aug. 3	Washington. Attend NCRP business meeting	KZM
Oct. 1	San Francisco. Confer with Dr. R. S. Stone, Univ. of Calif., on latent effects of β irradiation of skin	TGC
Oct. 2	San Francisco. Participate in Radiation Effects Working Group meeting	BRF TGC
Oct. 8-9	Cincinnati. Attend 10th Annual Bioassay and Analytical Chemistry Meeting	GWR
Oct. 19-23	ORNL. Meeting of ICRP Task Group on Standard Man	WSS
Nov. 3-6	Germantown. Attend 2nd AEC Conference on Radioactive Fallout from Nuclear Weapons Tests	RHB

<u>Date (1964)</u>	<u>Location and Purpose</u>	<u>Traveler*</u>
Nov. 11-12	Montreal. Attend meeting of ICRP Task Group on Lung Dynamics	BRF
Dec. 1	Hanford, Wash. Discussions with HAPO on internal β irradiation	TGC
Dec. 2-4	San Francisco. Attend American Nuclear Society and Radiation Effects Working Group meetings	TGC

* Initial abbreviations are: KZM - Dr. Karl Z. Morgan, WSS - Dr. Walter S. Snyder, BRF - Mr. Birney R. Fish, TGC - Mr. Thomas G. Clark, RHB - Mr. Rayford H. Boyett, GWR - Mr. George W. Royster, Jr.

10.0 REFERENCES

1. B. R. Fish and G. R. Patterson, Jr., "Preliminary Review of Potential Biological Hazards from Deposition of Nuclear Rocket Debris in the Earth Biosphere," ORNL-TM-501 (Classified), (1963).
2. R. H. Boyett, T. G. Clark and B. R. Fish, " β -Dosimetry Applications for Discrete Sources: I. Preliminary Review," ORNL-TM-802 (1964).
3. B. R. Fish, T. G. Clark, R. H. Boyett, W. C. McWhorter, and G. R. Royster, Jr., "Environmental Studies: Radiological Significance of Nuclear Rocket Debris - Annual Progress Report for Period Ending June 30, 1964," ORNL-TM-927 (Classified), (1964).
4. P. A. Thompson, S. A. Lewis, T. G. Clark, B. R. Fish and R. H. Boyett, "ZAP-I A Program to Calculate Radiation Dose Rates Near a Spherical Source," ORNL-TM-803 (1964).
5. P. A. Thompson, S. A. Lewis and T. G. Clark, "FORTRAN and CODAP Listings for ZAP-I," ORNL-TM-817 (1964).
6. J. M. Bridges, M. R. Trammell and W. S. Brown, "Radioactive Level of Small Particles Resulting from Operation and Destruct of the NERVA Reactor Core," WANL-TME-817 (1964), (Classified).
7. "Recommendations of the International Commission on Radiological Protection," British J. Radiology, Supplement 6, (1955).
8. G. N. Kenney, J. R. Cameron and D. Zimmerman, "Thermoluminescent Dosimeter Reading System," Rev. Sci. Instruments 34:7, 769 (1963).
9. D. B. Kochendorfer, "Calculated Activities of ^{235}U Fission Products for Very Short Nuclear Reactor Operation," USNRDL-TR-757 (1964).
10. W. L. Bond, "Making Small Spheres," Rev. Sci. Instr., 22:344 (1951).
11. J. A. Jenkins and M. McGeorge, "Control by Radium for Gastric Acidity," Arch. Int. Med. 70, 714 (1942).
12. M. McGeorge, "Results of Treatment of Gastric Hyperacidity by Radium, with Special Reference to Duodenal Ulceration," Quart. J. Med. 19, 111-128 (1950).
13. M. Pierce, "The Gastrointestinal Tract," Chapter 10, Histopathology of Irradiation from External and Internal Sources, W. Bloom, ed., McGraw-Hill, New York (1948).

14. H. Lisco, A. M. Brues, et al, "Carcinoma of the Colon in Rats following the Feeding of Radioactive Yttrium," (abstract), *Cancer Res.* 7, 721 (1947).
15. N. Simon, "Suppression of Gastric Acidity with Beta Particles of ^{32}P ," *Science* 109, 563-4 (1949).
16. R. F. Hedin, W. R. Miller, D. G. Jelatis, "Effect of Beta Irradiation on Gastric Acidity," *Arch. Surgery* 61, 748-757 (1950).
17. D. M. Douglas and W. R. Ghent, "Atrophy of the Gastric Glands Produced by Beta Rays," *Lancet*, p. 1035-1038 (June 3, 1950).
18. J. B. R. McKendry, "Intracavitary Visceral Irradiation: Effect on Gastric Acid Secretion," *Proc. Soc. Exp. Biol. and Med.* 75, 25-30 (1950).
19. W. Steinfield, "Suppression of Gastric Acidity by Radio-Krypton," *Proc. Soc. Exp. Biol and Med.* 81, 636-8 (1952).
20. B. W. Fox, A. Littman, et al, "Effect of Intra-gastric Irradiation on Gastric Acidity in the Dog," *Gastroenterology* 24, 517-534 (1953).
21. A. Littman, B. W. Fox, et al., "Lethal Effect of Intra-gastric Irradiation in the Dog," *Am. J. Physiol.* 174, 347-351 (1954).
22. W. E. Rothe and L. W. Tuttle, "Irradiation of the Gastrointestinal Tract by Insoluble Beta Emitters," UR-529, U. of Rochester Atomic Energy Project (1958).
23. R. C. Thompson and O. L. Hollis, "Irradiation of the Gastrointestinal Tract of the Rat by Ingested ^{106}Ru Ruthenium," *Am. J. Physiol.* 194, 308-12 (1958).
24. R. F. Palmer and M. F. Sullivan, "Effect of Intestinal Tract Irradiation on Serum Proteins of the Rat," *Proc. Soc. Exp. Biol. and Med.* 101, 326-8 (1959).
25. M. F. Sullivan, P. L. Hackett, et al., "Irradiation of the Intestine by Radioisotopes," *Rad. Res.* 13, 343-355 (1960).
26. M. F. Sullivan, S. Marks, et al., "X-Irradiation of Exteriorized or in situ Intestine of the Rat," *Rad. Res.* 11, 653-666 (1959).
27. M. M. Nold, R. L. Hayes and C. L. Comar, "Internal Radiation Dose Measurements in Live Experimental Animals," *Health Physics* 9, 915-920 (1963).

28. B. L. Hayes, J. E. Carlton and W. R. Butler, Jr., "Radiation Dose to the Human Intestinal Tract from Internal Emitters," *Health Physics* 9, 915-920 (1963).
29. M. C. Bell, "Effect of ^{144}Ce - ^{144}Pr Intestinal Irradiation of Sheep on ^{89}Sr and ^{45}Ca Metabolism," *Proc. 6th Int. Cong. on Nutrition*, Edinburgh, (1963).
30. University of Tennessee - Atomic Energy Commission - Agricultural Research Laboratory, Semi-Annual Progress Report, January-June 1964, ORO-625, p. 64.
31. M. C. Bell, personal communication.
32. M. F. Sullivan, S. Marks and R. C. Thompson, "Beta Irradiation of Rat Intestine," *Am. J. Path.* 43, 527-37 (1963).
33. I. S. Eve, "An outline of the Metabolism of Inhaled and Ingested Insoluble Radionuclides," *Brit. J. Radiol.* 37, 115-19 (1964).
34. A. F. McFee, "Effects of ^{144}Ce Administered to Pregnant Rats," *Proc. Soc. Exp. Biol. and Med.* 116, 712-15 (1964).
35. E. V. Hulse, "Intestinal Damage Produced by Beta Particles," *J. Path. Bact.* 76, 217-21 (1958).
36. O. M. Bizzell, et al., "Properties of Phosphorus-bakelite Beta Ray Sources," *Nucleonics* 8, 17-27 (1951).
37. R. S. Decker, Jr. and M. I. Goldman, "Particle Reentry Interactions," Nuclear Utilities Services, Washington, D.C., NUS-167 (1964).

10/10/10

10/10/10

Distribution

- | | |
|---------------------|----------------------------------|
| 1. A. M. Weinberg | 12. A. P. Fraas |
| 2. H. G. MacPherson | 13. A. J. Miller |
| 3. F. R. Bruce | 14. S. F. Carson |
| 4. W. H. Jordan | 15. C. E. Clifford |
| 5. K. Z. Morgan | 16. G. W. Parker |
| 6. W. S. Snyder | 17-18. Central Research Library |
| 7. T. J. Burnett | 19. Document Reference Section |
| 8. H. R. Boyett | 20-22. Laboratory Records |
| 9. T. G. Clark | 23. Laboratory Records (ORNL-RC) |
| 10. B. R. Fish | 24. ORNL Patent Office |
| 11. Wm. B. Cottrell | |
- 25-27. Paul Zigman, USNRDI, San Francisco, California.
28. Morton I. Goldman, Nuclear Utility Services, Inc. Washington, D. C.
29. Arnold B. Joseph, Office of Nuclear Safety, AEC/DRD, Washington D.C.
30. Joanne M. Bridges, Westinghouse Astronuclear Lab., Pittsburgh, Pa.
31. Paul M. Ordin, Space Nuclear Propulsion Office, NASA, Cleveland, O.
- 32-33. J. C. Whiton, H. Manning, P&VE-AN, National Aeronautics & Space Adm., Geo. G. Marshall Space Flight Center, Huntsville, Ala.
- 34-35. Ralph S. Decker, George P. Dix, Space Nuclear Propulsion Office AEC, Washington, D. C.
- 36-37. S. Allan Lough, H. D. Bruner, Division of Biology & Medicine, USAEC, Washington, D. C.
38. H. A. Kornberg, Battelle Northwest Laboratories, Richland, Wash.
- 39-40. L. P. D. King, W. H. Langham, Los Alamos Scientific Laboratory
41. R. C. Lee, Lockheed Missiles and Space Co., Sunnyvale, Calif.
- 42-56. Division of Technical Information Extension (DTIE)
57. Research and Development Division (ORO)
58. USAEC Headquarters Library, Washington, D. C.